Inorg. Chem. **2007**, *46*, 975–992

Replacement of Chlorides with Dicarboxylate Ligands in Anticancer Active Ru(II)-DMSO Compounds: A New Strategy That Might Lead to Improved Activity

Ioannis Bratsos,[†] Barbara Serli,[†] Ennio Zangrando,[†] Nikos Katsaros,[‡] and Enzo Alessio*[,†]

Dipartimento di Scienze Chimiche, Universitá di Trieste, Via L. Giorgieri 1, 34127 Trieste, Italy, and Institute of Physical Chemistry, NCSR Demokritos, 15310 Ag. Paraskevi, Athens, Greece

Received July 26, 2006

A series of new Ru(II)-DMSO complexes containing dicarboxylate ligands (dicarb), namely, oxalate (ox), malonate (mal), methylmalonate (mmal), dimethylmalonate (dmmal), and succinate (suc), have been synthesized and structurally characterized. These compounds were prepared from the known Ru(II)-Cl-DMSO anticancer complexes *cis*,*fac*-$[RuCl_2(DMSO\text{-}S)_3(DMSO\text{-}O)]$ (**1**) and *trans*-$[RuCl_2(DMSO\text{-}S)_4]$ (**2**) and from the chloride-free precursor *fac*-$[Ru(DMSO\text{-}S)_3(DMSO\text{-}O)_3][CF_3SO_3]_2$ (**3**), with the aim of assessing how the nature of the anionic ligands influences the biological activity of these species. Basically, the investigated ligands can be divided into two groups. The reaction of either **1** or **2** with K_2(dicarb) (dicarb = ox, mal, mmal) yielded preferentially the mononuclear species [K]*fac*-$[RuCl(DMSO\text{-}S)_3(\eta^2\text{-dicarb})]$ (dicarb = mal, **6**; mmal, **9**; ox, **14**) that contains a chelating dicarboxylate unit and a residual chloride. Likewise, when **3** was used as a precursor, the neutral mononuclear species *fac*-$[Ru(DMSO\text{-}O)(DMSO\text{-}S)_3(\eta^2\text{-dicarb})]$ (dicarb = mal, **7**; mmal, **10**; ox, **16**), which contains a DMSO-O ligand in the place of Cl^-, was obtained. On the contrary, K_2(suc) and K_2(dmmal) yielded preferentially the dinuclear species [*fac*-$Ru(DMSO\text{-}S)_3(H_2O)(\mu\text{-dicarb})]_2$ (dicarb = dmmal, **11**; suc, **13**), with two bridging dicarboxylate moieties. The two water molecules in anti geometry have strong intramolecular H-bonding with the non-coordinated oxygen atoms of the carboxylate groups. The solid-state X-ray structural data showed that the preferential binding mode of the investigated dicarboxylates, either bridging (μ) or chelating (η^2), is dictated mainly by steric reasons. Oxalate, unlike the other dicarboxylates, has also the bridging bis-chelate (η^4,μ) coordination mode available: this was found in the dinuclear species [{*fac*-$RuCl(DMSO\text{-}S)_3$}$_2(\eta^4,\mu$-ox)] (**15**) and [{*fac*-$Ru(DMSO\text{-}O)(DMSO\text{-}S)_3$}$_2(\eta^4,\mu$-ox)]$[CF_3SO_3]_2$ (**17**). We also isolated the unprecedented neutral metallacycle, [*fac*-$Ru(DMSO\text{-}S)_3(\eta^3,\mu\text{-ox})]_4$ (**18**), in which each oxalate unit has one unbound oxygen atom. The new complexes were thoroughly characterized by 1-D (^{1}H and ^{13}C) and 2-D (H–H– COSY and HMQC) NMR spectroscopy in solution and by IR spectroscopy in the solid state. The molecular structures of 10 compounds, **6**–**11**, **13**, **15**, **17**, and **18**, were determined by X-ray crystallography. The behavior of selected complexes in aqueous solution was investigated by ^{1}H NMR spectroscopy.

Introduction

In the last three decades, platinum-based drugs have played a crucial role in cancer chemotherapy.[1] The *cis*-$[PtCl_2(NH_3)_2]$ complex, known as *cisplatin*, is the first and still most widely used platinum drug.[2] The mechanism of action of *cisplatin* requires the dissociation of both chlorides, while the ammonia ligands remain tightly bound to the metal center. *Carboplatin*, $[Pt(cbdc)(NH_3)_2]$, a second-generation platinum drug that contains a chelating 1,1-cyclobutane dicarboxylate (cbdc) as an anionic leaving ligand instead of the two chlorides, has also been in wide clinical use since 1985.[3] *Carboplatin* is administered at significantly higher doses than *cisplatin* because it is less toxic, but it is also less potent.[2,3] The lower toxicity of *carboplatin* is related to the slower hydrolysis of the cbdc ligand as compared to the chlorides of *cisplatin*. Also *oxaliplatin*, [Pt(dach)(ox)] (dach = *R*,*R*-

* E-mail: alessi@units.it.
[†] Universitá di Trieste.
[‡] NCSR Demokritos.

(1) *Cisplatin: Chemistry and Biochemistry of a Leading Anticancer Drugs*; Lippert, B., Ed.; VHCA: Zürich, 1999.
(2) Wong, E.; Giandomenico, C. M. *Chem. Rev.* **1999**, *99*, 2451−2466.
(3) Lebwohl, D.; Canetta, R. *Eur. J. Cancer* **1998**, *34*, 1522−1534.

10.1021/ic0613964 CCC: $37.00
Published on Web 01/12/2007

1,2-diaminocyclohexane, ox = oxalate), a third-generation Pt complex that was recently approved for clinical use (routine treatment of colon cancer), contains a chelating dicarboxylate as a leaving ligand.[2]

Despite the widespread clinical use, chemotherapy with *cisplatin* and its analogues still has several drawbacks, in particular: (i) relatively narrow spectrum of activity, (ii) severe side-effects, and (iii) acquired resistance. These considerations have stimulated the search for new metal-based antitumor drugs.[4] Complexes of transition metals other than platinum may exhibit antitumor activity and toxic side-effects markedly different from that of Pt drugs for a number of obvious reasons: different chemical behavior, hydrolytic rates, and mechanism(s) of action. Among the several metals that are currently being investigated for their anticancer activity, ruthenium occupies a prominent position.[5] In particular, Ru-DMSO complexes appear to be promising antimetastatic agents: the Ru(III) compound [Him]*trans*-[$RuCl_4$(DMSO-S)(im)] (nicknamed NAMI-A, im = imidazole) developed by us, after extensive preclinical tests,[6] has accomplished phase I clinical trials and is scheduled to begin phase II trials soon.[7] Another Ru(III) complex developed by Keppler and co-workers, [Hind]*trans*-[$RuCl_4(ind)_2$] (KP 1019, ind = indazole), was recently introduced into clinical trials because of its activity against colorectal tumors in animal models.[8]

It is known that the chemical behavior of NAMI-A-type complexes ([LH]*trans*-[$RuCl_4$(DMSO-S)(L)], L = N ligand) in physiological aqueous solutions is dominated by the stepwise hydrolysis of at least two chlorides.[6] Chloride dissociation is the main chemical process that occurs also after the reduction of NAMI-A-type compounds to the corresponding Ru(II) species, a process that is likely to occur in vivo.[9]

We reasoned that, as for the case of Pt(II) anticancer drugs, also in active Ru-chloride-DMSO compounds, replacement of chlorides with carboxylates or chelating dicarboxylates is likely to induce significant differences in their hydrolytic behavior and, as a consequence, in their activity. A similar approach has been recently followed by the group of Reedijk that reported the synthesis and characterization of some dicarboxylato derivatives of cytotoxic Ru(II)-(2-phenylazopyridine) complexes.[10]

As Ru(III) is paramagnetic and limits the use of NMR spectroscopy for characterization purposes, we decided to start our investigation from Ru(II), rather than Ru(III)-DMSO complexes. In particular, we used as precursors the well-known Ru(II) isomers *cis*,*fac*-[$RuCl_2$(DMSO-S)$_3$(DMSO-O)] (**1**) and *trans*-[$RuCl_2$(DMSO-S)$_4$] (**2**) and their chloride-free derivative *fac*-[Ru(DMSO-S)$_3$(DMSO-O)$_3$][CF_3SO_3]$_2$ (**3**). Previous studies had shown that **1** and **2** exhibit antitumor and antimetastatic activity against animal tumor models even though at relatively high dosages only, owing to their low toxicity.[11,12]

Very little is known in the literature about the reactivity of Ru-chloride-DMSO complexes toward carboxylate and dicarboxylate ligands.[13] A complex with monodentate acetate ions, formulated as [Na]*fac*-[RuCl(DMSO-S)$_3$(O_2CCH_3)$_2$] (based on elemental analysis and IR spectrum), was apparently isolated upon treatment of **1** with sodium acetate in a methanol solution.[14] Reaction of **1** with silver acetate or trifluoroacetate in dichloromethane at room temperature afforded *fac*-[Ru(DMSO-S)$_3$(O_2CR)$_2$(H_2O)] (R = CH_3 or CF_3).[15] The X-ray structures showed that the two *cis*-monodentate carboxylate anions are strongly H-bonded, via their non-coordinated oxygen atoms, to the H_2O molecule that replaced the DMSO-O ligand in **1**.

Until our very recent report on Ru(II)-DMSO-cbdc compounds (cbdc = 1,1-cyclobutane dicarboxylate),[16] there were virtually no examples of Ru-DMSO complexes with potentially chelating dicarboxylates, with the exception of the dinuclear species with a bridging bis-bidentate oxalate ligand, [{*fac*-RuCl(DMSO-S)$_3$}$_2$(η^4,μ-ox)] and [{*cis*-Ru(CH_3-CN)Cl(DMSO-S)$_2$}$_2$(η^4,μ-ox)], which were serendipitously obtained in low yield by treatment of **1** with substituted

(4) (a) Guo, Z.; Sadler, P. J. *Angew. Chem., Int. Ed.* **1999**, *38*, 1512−1531. (b) Clarke, M. J. *Coord. Chem. Rev.* **2002**, *232*, 69−93. (c) Zhang, C. X.; Lippard, S. J. *Curr. Opin. Chem. Biol.* **2003**, *7*, 481−489.

(5) (a) Clarke, M. J.; Zhu, F.; Frasca, D. R. *Chem. Rev.* **1999**, *99*, 2511−2533. (b) Allardyce, C. S.; Dyson, P. J. *Platinum Metals Rev.* **2001**, *45*, 62−69. (c) Clarke, M. J. *Coord. Chem. Rev.* **2003**, *236*, 209−233. (d) Yan, Y. K.; Melchart, M.; Habtemariam, A.; Sadler, P. J. *Chem. Commun.* **2005**, 4764−4776. (e) Dyson, P. J.; Sava, G. *Dalton Trans.* **2006**, 1929−1933.

(6) (a) Sava, G.; Alessio, E.; Bergamo, A.; Mestroni, G. In *Topics in Biological Inorganic Chemistry, Volume 1: Metallo-pharmaceuticals*; Clarke, M. J., Sadler, P. J., Eds.; Springer: Berlin, 1999; pp 143−169. (b) Alessio, E.; Mestroni, G.; Bergamo, A.; Sava, G. In *Metal Ions in Biological Systems, Vol. 42: Metal Ions and Their Complexes in Medication and in Cancer Diagnosis and Therapy*; Sigel, A., Sigel, H., Eds.; M. Dekker: New York, 2004; pp 323−351. (c) Alessio, E.; Mestroni, G.; Bergamo, A.; Sava, G. *Curr. Topics Med. Chem.* **2004**, *4*, 1525−1535.

(7) Redemaker-Lakhai, J. M.; van den Bongard, D.; Pluim, D.; Beijnen, J. H.; Schellens, J. H. M. *Clin. Cancer Res.* **2004**, *10*, 3717−3727.

(8) Reisner, E.; Arion, V. B.; Guedes da Silva, M. F. C.; Lichtenecker, R.; Eichinger, A.; Keppler, B. K.; Kukushkin, V. Y.; Pombeiro, A. J. L. *Inorg. Chem.* **2004**, *43*, 7083−7093 and references therein.

(9) Sava, G.; Bergamo, A.; Zorzet, S.; Gava, B.; Casarsa, C.; Cocchietto, M.; Furlani, A.; Scarcia, V.; Serli, B.; Iengo, E.; Alessio, E.; Mestroni, G. *Eur. J. Cancer* **2002**, *38*, 427−435.

(10) Hotze, A. C. G.; Bacac, M.; Velders, A. H.; Jansen, B. A. J.; Kooijman, H.; Spek, A. L.; Haasnoot, J. G.; Reedijk, J. *J. Med. Chem.* **2003**, *46*, 1743−1750.

(11) (a) Alessio, E.; Xu, Y.; Cauci, S.; Mestroni, G.; Quadrifoglio, F.; Viglino, P.; Marzilli, L. G. *J. Am. Chem. Soc.* **1989**, *111*, 7068−7071. (b) Sava, G.; Pacor, S.; Zorzet, S.; Alessio, E.; Mestroni G. *Pharmacol. Res.* **1989**, *21*, 617−628. (c) Sava, G.; Pacor, S.; Bregant, F.; Ceschia, V.; Luxich, E.; Alessio, E.; Mestroni, G. *Pharmacol. (Life Sci. Adv.)* **1990**, *9*, 79−84. (d) Loseto, F.; Alessio, E.; Mestroni, G.; Lacidogna, G.; Nassi, A.; Giordano, D.; Coluccia M. *Anticancer Res.* **1991**, *11*, 1549−1554. (e) Colucci, M.; Coluccia, M.; Montemurro, P.; Conese, M.; Nassi, A.; Loseto, F.; Alessio, E.; Mestroni, G.; Semeraro N. *Int. J. Oncol.* **1993**, *2*, 527−529. (f) Mestroni, G.; Alessio, E.; Sava, G.; Pacor, S.; Coluccia, M. In *Metal Complexes in Cancer Chemotherapy*; Keppler, B. K., Ed.; VCH Verlag: Weinheim, 1993; pp 159−185. (g) Coluccia, M.; Sava, G.; Loseto, F.; Nassi, A.; Boccarelli, A.; Giordano, D.; Alessio, E.; Mestroni, G. *Eur. J. Cancer* **1993**, *29*, 1873−1879.

(12) Brindell, M.; Kulis, E.; Elmroth, S. K. C.; Urbanska, K.; Stochel, G. *J. Med. Chem.* **2005**, *48*, 7298−7304.

(13) Alessio, E. *Chem. Rev.* **2004**, *104*, 4203−4242.

(14) Buslaeva, T. M.; Rudnitskaya, O. V.; Kabanova, A. G.; Fedorova, G. A. *Russ. J. Coord. Chem.* **2000**, *26*, 429−432.

(15) Malik, K. Z.; Robinson, S. D.; Steed, J. W. *Polyhedron* **2000**, *19*, 1589−1592.

(16) Bratsos, I.; Zangrando, E.; Serli, B.; Katsaros, N.; Alessio, E. *Dalton Trans.* **2005**, 3881−3885.

Scheme 1. Reactivity of **1** toward K_2(cbdc)

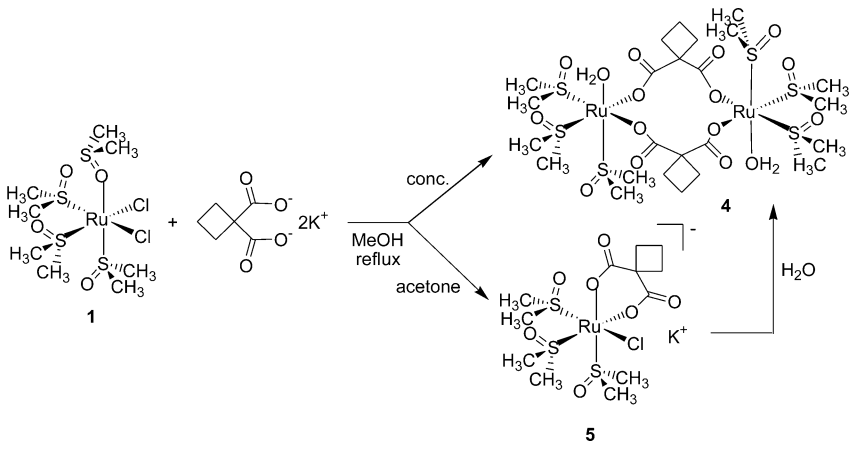

squarates that underwent decomposition.[17] Recently, the [Ru(DMSO-S)(η^2-mal)(tpy)] and [Ru(DMSO-S)(η^2-ox)(tpy)] compounds (tpy = 2,2′:6′,2″-terpyridyne; mal = malonate; ox = oxalate) were structurally characterized in the solid state.[18]

We found that the thermodynamic product of the reaction between **1** and K_2(cbdc) in a number of different reaction conditions is the dinuclear species [*fac*-Ru(DMSO-S)$_3$(H_2O)-(μ-cbdc)]$_2$ (**4**) (Scheme 1), in which two *fac*-Ru(DMSO-S)$_3$ fragments are held together by two bridging cbdc units.[16] The two water molecules, in anti geometry, make strong intramolecular H-bonds with the non-coordinated oxygen atoms of the carboxylate groups, similar to those found in *fac*-[Ru(DMSO-S)$_3$(O_2CR)$_2$(H_2O)] (R = CH_3 or CF_3).[15]

This coordination mode of the cbdc anion was unprecedented, as this ligand usually behaves as a chelate (η^2-cbdc) on square planar metal centers and also on most octahedral metal centers, including Ru.[10,19] Actually, the mononuclear anionic complex with a chelating cbdc unit, [K]*fac*-[Ru(DMSO-S)$_3$Cl(η^2-cbdc)] (**5**), could be isolated as an intermediate in the preparation of **4** (Scheme 1).[16] In aqueous solutions, Cl^- dissociation from **5** is accompanied by a rearrangement in the coordination mode of cbdc from chelate (η^2, **5**) to bridging (μ, **4**), thus implying that **4** is thermodynamically more stable than **5**.

Intrigued by our results with cbdc,[16] we extended our investigation to other simple dicarboxylate ligands, normally employed also in Pt anticancer drugs (Chart 1):[1−3,20] oxalate (ox, $^-$OOC-COO$^-$), malonate (mal, $^-$OOC-CH_2-COO$^-$), methylmalonate (mmal, $^-$OOC-CH(CH_3)-COO$^-$), and dimethylmalonate (dmmal, $^-$OOC-C(CH_3)$_2$-COO$^-$), which are structurally very similar to cbdc with either protons or methyl groups replacing the four-membered ring on C^1, and succinate (suc, $^-$OOC-(CH_2)$_2$-COO$^-$), which has a longer carbon chain.

Chart 1

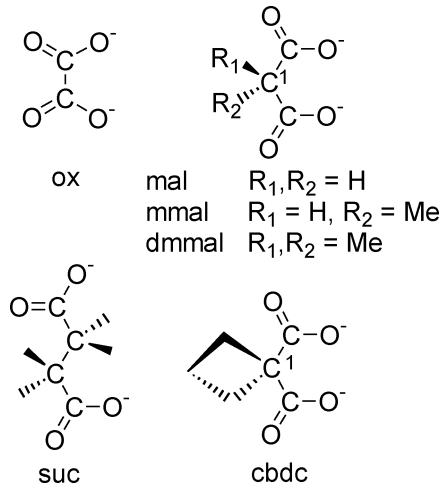

Other than in the field of anticancer metal complexes, dicarboxylate ligands are also extensively investigated as building blocks for the design of new materials with hybrid organic−inorganic frameworks.[21] In particular, the ability of carboxylato bridges to mediate significant ferro- or antiferromagnetic interactions between paramagnetic metal ions has stimulated studies on structural and magnetic properties of polynuclear complexes of transition metals (mainly extended 2-D and 3-D structures), aimed at the design of new molecular materials exhibiting unusual magnetic properties.

In this paper, we describe a number of new Ru(II)-DMSO complexes (mono-, di-, and tetra-nuclear) obtained by the treatment of precursors **1**−**3** with these dicarboxylates. The complexes were thoroughly characterized by means of 1-D and 2-D NMR (^{1}H, ^{13}C, H− H COSY, and HMQC) and IR spectroscopies, and the molecular structures of 10 of them were determined by X-ray crystallography. The chemical behavior of selected complexes in aqueous solution was studied (by ^{1}H NMR spectroscopy) in view of their potential antitumor activity.

(17) Piggot, P. M. T.; Hall, L. A.; White, A. J. P.; Williams, D. J. *Inorg. Chim. Acta* **2004**, *357*, 250−258.
(18) (a) Rack, J. J.; Rachford, A. A.; Shelker, A. M. *Inorg. Chem.* **2003**, *42*, 7357−7359. (b) Rachford, A. A.; Petersen, J. L.; Rack, J. J. *Inorg. Chem.* **2005**, *44*, 8065−8075.
(19) Davies, D. L.; Fawcett, J.; Krafczyk, R.; Russell, D. R.; Singh, K. *J. Chem. Soc., Dalton Trans.* **1998**, 2349−2352.
(20) (a) Khokhar, A. R.; Lumetta, G. J. *Inorg. Chim. Acta* **1988**, *153*, 255−259. (b) Cleare, M. J.; Hoeschele, J. D. *Bioinorg. Chem.* **1973**, *2*, 187−210.
(21) (a) Rao, C. N. R.; Natarajan, S.; Vaidhyanathan, R. *Angew. Chem., Int. Ed.* **2004**, *43*, 1466−1496. (b) Perles, J.; Iglesias, M.; Ruiz-Valero, C.; Snejko, N. *Chem. Commun.* **2003**, 346−347 and references therein.

Experimental Procedures

Materials. Oxalic acid dihydrate, malonic acid, methylmalonic acid, dimethylmalonic acid, and succinic acid were purchased from Sigma. The potassium salts of the ligands were obtained by treatment of the respective acids with excess KOH in ethanol. The silver salt of malonate, Ag_2(mal), was obtained by treatment of K_2(mal) with $AgNO_3$ in water. All the reagents and solvents were used without further purification. *cis*,*fac*-[$RuCl_2$(DMSO-S)$_3$(DMSO-O)] (**1**),[22] *trans*-[$RuCl_2$(DMSO-S)$_4$] (**2**),[22] *fac*-[Ru(DMSO-S)$_3$-(DMSO-O)$_3$][CF_3SO_3]$_2$ (**3**),[23] [*fac*-Ru(DMSO-S)$_3$(H_2O)(μ-cbdc)]$_2$ (**4**),[16] and [K]*fac*-[RuCl(DMSO-S)$_3$(η^2-cbdc)] (**5**)[16] were prepared following published procedures.

Instrumental Methods. ^{1}H and ^{13}C NMR spectra were recorded at 400 and 100.5 MHz, respectively, on a JEOL Eclipse 400FT spectrometer; the 2-D experiments (H−H COSY, HMQC (heteronuclear multiple-quantum coherence)) were recorded at 500 MHz on a Bruker Avance instrument. All spectra were run at room temperature (r.t.), unless otherwise stated. ^{1}H and ^{13}C chemical shifts in D_2O were referenced to the internal standard sodium 3-(trimethylsilyl−)-1-propanesulfonate (TSP) at $\delta = 0.00$. For the hydrolysis experiments, 5 mM solutions of each complex were prepared, both in pure D_2O and in 100 mM NaCl/D_2O, and were monitored in time by ^{1}H NMR spectroscopy. In addition, after the establishment of the hydrolysis equilibrium in D_2O, a 10 μL volume of a 5 M NaCl solution in D_2O was added (so that the final concentration of NaCl was 100 mM), and the ^{1}H NMR spectrum was recorded immediately afterward. Infrared spectra were recorded on a Perkin-Elmer 983G spectrometer. Elemental analysis was performed at the Dipartimento di Scienze Chimiche, University of Trieste.

Synthesis of the Complexes. Most of the complexes were successfully synthesized following various alternative routes. Herein, we report the most efficient and easy procedure for each one.

[K]*fac*-[RuCl(DMSO-S)$_3$(η^2-mal)] (6). K_2(mal) (36 mg, 0.20 mmol) was added to a warm stirred solution of *cis*,*fac*-[$RuCl_2$-(DMSO-S)$_3$(DMSO-O)] (**1**, 97 mg, 0.20 mmol) in methanol (10 mL). The solution mixture was refluxed for 1 h and then concentrated in vacuo to approximately 3 mL. Slow evaporation of the solution to approximately 0.5 mL afforded yellow square crystals suitable for X-ray analysis that were removed by filtration, washed with acetone, and vacuum-dried at room temperature. Yield 72.2 mg (66%). Anal. Calcd for $C_9H_{20}ClKO_7RuS_3 \cdot 2H_2O$ (M_r 548.08): C, 19.7; H, 4.41. Found: C, 19.4; H, 4.22. Compound **6** is very soluble in water, soluble in DMSO, DMF, slightly soluble in methanol, and insoluble in a number of solvents such as ethanol, acetone, dichloromethane, chloroform, and THF. ^{1}H NMR (D_2O, δ ppm): 4.01 (d, 1H, $J = 18.3$ Hz, C^1H_a), 3.42 (s, 6H, DMSO-S), 3.39 (s, 6H, DMSO-S), 3.21 (s, 6H, DMSO-S), 3.15 (d, 1H, $J = 18.3$ Hz, C^1H_b). ^{13}C{^{1}H} NMR (D_2O, δ ppm): 181.6 (*C*OO), 48.3 (*C*H$_3$, DMSO-S), 47.6 (*C*^{1}H$_2$), 46.3 (*C*H$_3$, DMSO-S), 45.8 (*C*H$_3$, DMSO-S). Selected IR (KBr, cm^{-1}): $\nu_{asym(COO)}$ 1575 (s); $\nu_{sym(COO)}$ 1414 (s); $\nu_{S=O}$ 1110 (s); ν_{Ru-S} 422 (s). UV−vis spectrum (λ_{max}, nm (ϵ, M^{-1} cm^{-1})): 297 (816), 342 (722).

***fac*-[Ru(DMSO-S)$_3$(DMSO-O)(η^2-mal)] (7).** To a solution of *fac*-[Ru(DMSO-S)$_3$(DMSO-O)$_3$][CF_3SO_3]$_2$ (**3**, 87 mg, 0.10 mmol) in a DMSO/methanol (1:2) mixture (3 mL), K_2(mal) was added (36 mg, 0.20 mmol). The solution was refluxed for 1 h. Methanol was then removed in vacuo and replaced with acetone (ca. 3 mL). Colorless square crystals of **7** suitable for X-ray analysis formed within ca. 24 h and were removed by filtration, washed with acetone, and vacuum-dried at room temperature. Yield 45 mg (87%). Anal. Calcd for $C_{11}H_{26}O_8RuS_4$ (M_r 515.63): C, 25.6; H, 5.08. Found: C, 25.5; H, 4,68. This complex is soluble in water, methanol, chloroform, slightly soluble in ethanol, DMSO, and DMF, and insoluble in acetone and THF. ^{1}H NMR (D_2O, δ ppm): 3.85 (d, 1H, $J = 18.3$ Hz, C^1H_a), 3.42 (d, 1H, $J = 18.3$ Hz, C^1H_b), 3.35 (s, 12H, DMSO-S), 3.34 (s, 6H, DMSO-S), 2.84 (s, 6H, DMSO-O). ^{13}C{^{1}H} NMR (D_2O, 278 K, δ ppm): 181.4 (*C*OO), 48.6 (*C*H$_3$, DMSO-S), 48.2 (*C*^{1}H$_2$), 46.6 (*C*H$_3$, DMSO-S), 45.9 (*C*H$_3$, DMSO-S), 39.7 (*C*H$_3$, DMSO-O). Selected IR (KBr, cm^{-1}): $\nu_{asym(COO)}$ 1613 (vs); $\nu_{sym(COO)}$ 1375 (s); $\nu_{S=O}$ (DMSO-S) 1106 (s); $\nu_{S=O}$ (DMSO-O) 925 (s); ν_{Ru-O} 479 (w); ν_{Ru-S} 425 (m). UV−vis spectrum (λ_{max}, nm (ϵ, M^{-1} cm^{-1})): 290 (622), 328 (584).

[*fac*-Ru(DMSO-S)$_3$(H_2O)(μ-mal)]$_2$ (8). Ag_2(mal) (153 mg, 0.48 mmol) was added to a magnetically stirred solution of **1** (200 mg, 0.41 mmol) in dichloromethane (10 mL). The mixture was stirred overnight at room temperature in the dark. AgCl was filtered off, and the very pale yellow solution was concentrated in vacuo to approximately 5 mL. Slow evaporation afforded colorless crystals that were removed by filtration, washed with methanol and acetone, and then vacuum-dried at room temperature. Yield 68 mg (36%). Crystals suitable for X-ray analysis were obtained by recrystallization from methanol. Anal. Calcd for $C_{18}H_{44}O_{16}Ru_2S_6$ (M_r 911.06): C, 23.7; H, 4.87. Found: C, 23.8; H, 4.88. This complex is soluble in water and chloroform, slightly soluble in methanol and nitromethane, and insoluble in DMSO, ethanol, acetone, dichloromethane, DMF, THF, and acetonitrile. ^{1}H NMR (D_2O, δ ppm): 3.35 (s, 12H, DMSO-S), 3.34 (s, 4H, C$^1H_2$), 3.32 (s, 12H, DMSO-S), 3.29 (s, 12H, DMSO-S). ^{13}C{^{1}H} NMR (D_2O, δ ppm): 183.8 (*C*OO), 52.6 (*C*^{1}H$_2$), 47.9 (*C*H$_3$, DMSO-S), 47.0 (*C*H$_3$, DMSO-S), 45.3 (*C*H$_3$, DMSO-S). Selected IR (KBr, cm^{-1}): $\nu_{asym(COO)}$ 1582 (s); $\nu_{sym(COO)}$ 1360 (s); $\nu_{S=O}$ 1094 (s); ν_{Ru-S} 431 (m). UV−vis spectrum (λ_{max}, nm (ϵ, M^{-1} cm^{-1})): 284 (1263), 325 (1155).

[K]*fac*-[RuCl(DMSO-S)$_3$(η^2-mmal)] (9). K_2(mmal) (38.9 mg, 0.20 mmol) was added to **1** (97 mg, 0.20 mmol) partially dissolved in methanol (10 mL). The mixture was refluxed for 2 h, obtaining a yellow−orange solution. Concentration of the solvent to ca. 5 mL and addition of ethanol (5 mL) induced the formation of white solid (KCl), which was removed by filtration. Slow evaporation of the yellow solution to approximately 2 mL gave rise to the formation of **9** as a pale yellow solid, which was collected by filtration, washed with ethanol, acetone, and diethyl ether, and vacuum-dried. Yield 52.0 mg (49%). Crystals suitable for X-ray analysis were obtained by slow diffusion of acetone into a methanol solution of **9**. Anal. Calcd for $C_{10}H_{22}ClKO_7RuS_3$ (M_r 526.10): C, 22.8; H, 4.21. Found: C, 22.0; H, 4.40. Complex **9** is soluble in water and DMSO, slightly soluble in methanol and ethanol, and insoluble in acetone, dichloromethane, chloroform, nitromethane, and acetonitrile. ^{1}H NMR (D_2O, δ ppm): 4.31 (m, 1H, $J = 7.1$ Hz, C^1H), 3.43 (s, 6H, DMSO-S), 3.39 (s, 6H, DMSO-S), 3.16 (s, 6H, DMSO-S), 1.13 (d, 3H, $J = 7.1$ Hz, C$H_{3(mmal)}$). ^{13}C{^{1}H} NMR (10% D_2O, δ ppm): 181.6 (*C*OO), 49.1 (*C*^{1}H, mmal), 46.3 (*C*H$_3$, DMSO-S), 44.5 (*C*H$_3$, DMSO-S), 43.8 (*C*H$_3$, DMSO-S), 13.9 (*C*H$_3$, mmal). Selected IR (KBr, cm^{-1}): $\nu_{asym(COO)}$ 1610 (s), 1587 (s); $\nu_{sym(COO)}$ 1413 (s); $\nu_{S=O}$ 1106 (s); ν_{Ru-S} 425 (s). UV−vis spectrum (λ_{max}, nm (ϵ, M^{-1} cm^{-1})): 310 (318), 360 (508).

***fac*-[Ru(DMSO-S)$_3$(DMSO-O)(η^2-mmal)] (10).** To a solution of **3** (87 mg, 0.10 mmol) in a DMSO/methanol (1:5) mixture (3 mL), K_2(mmal) was added (36 mg, 0.20 mmol). The solution was

(22) Alessio, E.; Mestroni, G.; Nardin, G.; Attia, W. M.; Calligaris, M.; Sava, G.; Zorzet, S. *Inorg. Chem.* **1988**, *27*, 4099−4106.
(23) Iengo, E.; Zangrando, E.; Baiutti, E.; Munini, F.; Alessio, E. *Eur. J. Inorg. Chem.* **2005**, 1019−1031.

Table 1. Crystallographic Data for Compounds **6**−**10**

	6·2H_2O	**7**	**8**	**9**·1.5H_2O	**10**·H_2O
empirical formula	$C_9H_{24}ClKO_9RuS_3$	$C_{11}H_{26}O_8RuS_4$	$C_{18}H_{44}O_{16}Ru_2S_6$	$C_{10}H_{25}ClKO_{8.5}RuS_3$	$C_{12}H_{30}O_9RuS_4$
fw	548.08	515.63	911.03	553.10	547.67
cryst system	monoclinic	monoclinic	triclinic	monoclinic	monoclinic
space group	*Pn*	$P2_1/n$	$P\bar{1}$	$P2_1/n$	*Cc*
a (Å)	8.930(3)	8.992(2)	8.825(2)	10.423(3)	13.807(3)
b (Å)	8.369(3)	13.819(4)	13.695(4)	13.419(2)	10.937(2)
c (Å)	13.229(4)	16.524(4)	14.235(4)	15.131(3)	14.872(3)
α (deg)			85.88(2)		
β (deg)	90.67(2)	103.09(3)	88.71(2)	99.79(2)	103.21(2)
γ (deg)			81.67(3)		
V (Å^3)	988.6(6)	1999.9(9)	1697.7(8)	2085.5(8)	2186.4(8)
Z	2	4	2	4	4
D_{calcd} (g cm^{-3})	1.841	1.713	1.782	1.762	1.664
μ (Mo Kα) (mm^{-1})	1.492	1.234	1.323	1.414	1.137
F(000)	556	1056	928	1124	1128
θ range (deg)	2.77−30.55	1.94−27.47	1.43−29.62	2.04−27.10	2.40−31.06
reflns	12195	25413	23240	24135	26261
ind reflns	5007	4235	8687	4430	6866
R_{int}	0.0324	0.0508	0.0380	0.0392	0.0450
reflns ($I > 2\ \sigma(I)$)	4777	3218	5850	3464	5499
refined params	230	225	403	226	241
GOF (F^2)	1.078	1.051	0.907	1.113	0.913
R1 ($I > 2\sigma(I)$)[a]	0.0347	0.0514	0.0372	0.0537	0.0363
wR2[a]	0.0969	0.1391	0.0939	0.1695	0.0777
Flack param	0.01(3)				−0.01(3)
residuals (e/Å^3)	0.687, −0.630	0.907, −1.023	0.608, −0.370	1.295, −0.586	0.414, −0.435

[a] $R1 = \Sigma||F_o| - |F_c||/\Sigma|F_o|$, $wR2 = [\Sigma w(F_o^2 - F_c^2)^2/\Sigma w(F_o^2)^2]^{1/2}$.

Table 2. Crystallographic Data for Compounds **11**, **13**, **15**, **17**, and **18**

	11·H_2O	**13**·2EtOH[a]	**15**	**17**	**18**·5H_2O
empirical formula	$C_{22}H_{54}O_{17}Ru_2S_6$	$C_{24}H_{60}O_{18}Ru_2S_6$	$C_{14}H_{36}Cl_2O_{10}Ru_2S_6$	$C_{20}H_{48}F_6O_{18}Ru_2S_{10}$	$C_{32}H_{72}O_{28}Ru_4S_{12}$
fw	985.15	1031.22	829.83	1213.32	1783.98
cryst system	triclinic	triclinic	triclinic	triclinic	tetragonal
space group	$P\bar{1}$	$P\bar{1}$	$P\bar{1}$	$P\bar{1}$	$I4_1/a$
a (Å)	8.553(3)	8.336(3)	8.446(2)	13.345(4)	14.192(3)
b (Å)	11.356(3)	9.723(3)	8.548(2)	13.192(3)	
c (Å)	22.512(4)	13.185(5)	10.609(3)	13.618(4)	33.548(5)
α (deg)	79.08(3)	102.45(4)	90.16(3)	109.26(3)	
β (deg)	82.26(2)	101.29(5)	74.63(2)	93.02(2)	
γ (deg)	69.96(2)	95.31(4)	80.47(2)	92.23(3)	
V (Å^3)	2011.2(10)	1013.1(6)	727.5(3)	2256.0(11)	6757(2)
Z	2	1	1	2	4
D_{calcd} (g cm^{-3})	1.627	1.690	1.894	1.786	1.754
μ (Mo Kα) (mm^{-1})	1.125	9.524	1.696	1.219	1.328
F(000)	1012	532	418	1228	3624
θ range (deg)	1.93−27.48	3.52−64.79	2.42−31.06	1.59−25.03	2.36−26.72
reflns	26261	14863	10817	25113	36607
ind reflns	8260	3108	4191	7250	3589
R_{int}	0.0295	0.0740	0.0286	0.0887	0.0705
reflns ($I > 2\ \sigma(I)$)	6805	2701	3329	2880	2182
refined params	445	235	160	505	192
GOF (F^2)	1.026	1.132	0.970	0.826	0.980
R1 ($I > 2\sigma(I)$)[b]	0.0430	0.0729	0.0374	0.0691	0.0599
wR2[b]	0.1326	0.2314	0.1014	0.1615	0.1507
Flack param	1.378, −0.396	1.358, −0.864	0.513, −1.095	1.275, −0.889	1.316, −0.489

[a] Data collected using Cu Kα radiation. [b] $R1 = \Sigma||F_o| - |F_c||/\Sigma|F_o|$, $wR2 = [\Sigma w(F_o^2 - F_c^2)^2/\Sigma w(F_o^2)^2]^{1/2}$.

refluxed for 1 h. Methanol was then removed in vacuo, thus inducing partial precipitation of **10** as a microcrystalline solid in the DMSO solution. Addition of acetone (ca. 1.5 mL) accomplished the precipitation within 24 h. The solid was collected by filtration, washed with acetone, and vacuum-dried at room temperature. Yield: 33.6 mg (63%). Colorless square plates of **10** suitable for X-ray analysis were obtained, in lower yield, from the same procedure using a larger volume of DMSO (e.g., 1 mL). Anal. Calcd for $C_{12}H_{28}O_8RuS_4$ (M_r 529.68): C, 27.2; H, 5.33. Found: C, 26.8; H, 5.47. Complex **10** is soluble in water and methanol, slightly soluble in DMSO, nitromethane, ethanol, and chloroform, and insoluble in acetone, dichloromethane, and acetonitrile. ^{1}H NMR (D_2O, *δ* ppm): 3.84 (m, 1H, $J = 6.9$ Hz, C^1*H*), 3.43 (s, 6H, DMSO-S), 3.34 (s, 6H, DMSO-S), 3.33 (s, 6H, DMSO-S), 2.82 (s, 6H, DMSO-O), 1.24 (d, 3H, $J = 6.9$ Hz, C$H_{3(mmal)}$). Selected IR (KBr, cm^{-1}): $\nu_{asym(COO)}$ 1608 (s), 1592 (s); $\nu_{sym(COO)}$ 1396 (s); $\nu_{S=O}$ (DMSO-S) 1108 (s); $\nu_{S=O}$ (DMSO-O) 926 (s); ν_{Ru-O} 487 (m); ν_{Ru-S} 430 (s). UV−vis spectrum (λ_{max}, nm (ϵ, M^{-1} cm^{-1})): 292 (573), 328 (546).

[*fac*-Ru(DMSO-S)$_3$(H$_2$O)(*μ*-dmmal)]$_2$ (11). K_2(dmmal) (41.7 mg, 0.20 mmol) was added to **1** (97 mg, 0.20 mmol) partially dissolved in methanol (10 mL). The mixture was refluxed for 2 h, obtaining a yellow−orange solution. Slow evaporation of the solvent to approximately 2 mL afforded yellow crystals suitable for X-ray

analysis that were collected by filtration, washed with cold methanol, acetone, and diethyl ether, and vacuum-dried. Yield 61.0 mg (63%). Anal. Calcd for $C_{22}H_{52}O_{16}Ru_2S_6$ (M_r 967.17): C, 27.3; H, 5.42. Found: C, 26.7; H, 5.47. Complex **11** is soluble in water, slightly soluble in dichloromethane and chloroform, and insoluble in methanol, ethanol, DMSO, acetone, nitromethane, and acetonitrile. ^{1}H NMR (D_2O, δ ppm): 3.33 (s, 12H, DMSO-S), 3.32 (s, 12H, DMSO-S), 3.30 (s, 12H, DMSO-S), 1.39 (s, 12H, C$H_{3(dmmal)}$). ^{13}C{^{1}H} NMR (D_2O, δ ppm): 186.8 (*C*OO, dmmal), 54.7 (C^1, dmmal), 45.3 (*C*H_3, DMSO-S), 44.4 (*C*H_3, DMSO-S), 43.3 (*C*H_3, DMSO-S), 23.4 (*C*H_3, dmmal). Selected IR (KBr, cm^{-1}): $\nu_{asym(COO)}$ 1586 (s); $\nu_{sym(COO)}$ 1408 (s); $\nu_{S=O}$ 1118 (s); ν_{Ru-S} 428 (s). UV−vis spectrum (λ_{max}, nm (ϵ, M^{-1} cm^{-1})): 284 (796), 327 (785).

[K]*fac*-[RuCl(DMSO-S)$_3$(η^2-dmmal)] (12). K_2(dmmal) (41.7 mg, 0.20 mmol) was added to **1** (97 mg, 0.20 mmol) partially dissolved in methanol (10 mL). The mixture was refluxed for 3 h yielding, after ca. 10 min, a yellow solution. Removal of methanol in vacuo yielded an oil, and addition of ethanol induced the formation of white solid (KCl) that was removed by filtration. The yellow filtrate was rotary-evaporated to dryness yielding an oil, which was treated with acetone to form a pale yellow solid that was removed by filtration, washed with cold acetone and dichloromethane, and vacuum-dried. Yield 86.9 mg (80%). Anal. Calcd for $C_{11}H_{24}ClKO_7RuS_3$ (M_r 540.12): C, 24.5; H, 4.48. Found: C, 23.9; H, 4.52. Complex **12** is soluble in water, methanol, ethanol, and DMSO, slightly soluble in acetone, and insoluble in dichloromethane, chloroform, nitromethane, and acetonitrile. ^{1}H NMR (D_2O, δ ppm): 3.42 (s, 6H, DMSO-S), 3.42 (s, 6H, DMSO-S), 3.26 (s, 6H, DMSO-S), 1.47 (s, 3H, $C_aH_{3(dmmal)}$), 1.13 (s, 3H, $C_bH_{3(dmmal)}$). ^{13}C{^{1}H} NMR (D_2O, δ ppm): 187.2 (*C*OO), 53.1 (C^1, dmmal), 46.0 (*C*H_3, DMSO-S), 44.0 (*C*H_3, DMSO-S), 43.8 (*C*H_3, DMSO-S), 28.4 (C_aH_3, dmmal), 26.3 (C_bH_3, dmmal). Selected IR (KBr, cm^{-1}): $\nu_{asym(COO)}$ 1581 (s), 1562 (s), 1538 (s); $\nu_{sym(COO)}$ 1411 (s); $\nu_{S=O}$ 1106 (s); ν_{Ru-S} 424 (m). UV−vis spectrum (λ_{max}, nm (ϵ, M^{-1} cm^{-1})): 297 (412), 333 (393).

[*fac*-Ru(DMSO-S)$_3$(H$_2$O)(μ-suc)]$_2$ (13). K_2(suc) (40 mg, 0.21 mmol) was added to **1** (100 mg, 0.21 mmol) partially dissolved in methanol (7 mL). The mixture was refluxed for 2 h, obtaining a yellow solution. Slow evaporation of the solvent to approximately 1 mL afforded a yellow solid that was collected by filtration, washed with ethanol and diethyl ether, and vacuum-dried. Yield: 53.6 mg (54%). Recrystallization from DMSO-ethanol gave crystals suitable for X-ray analysis. Anal. Calcd for $C_{20}H_{48}O_{16}Ru_2S_6$ (M_r 939.12): C, 25.8; H, 5.15. Found: C, 24.8; H, 5.20. Complex **13** is soluble in water, slightly soluble in methanol, dichloromethane, chloroform, DMSO, DMF, nitromethane, and acetonitrile, and insoluble in ethanol, acetone, THF, and hexanes. ^{1}H NMR (D_2O, δ ppm): 3.30 (s, 12H, DMSO-S), 3.29 (s, 12H, DMSO-S), 3.28 (s, 12H, DMSO-S), 2.75 (d, 4H, J = 14.7 Hz, C^1H_a + C^2H_a), 2.56 (d, 4H, J = 14.7 Hz, C^1H_b + C^2H_b). ^{13}C{^{1}H} NMR (D_2O, δ ppm): 188.1 (*C*OO), 45.3 (*C*H_3, DMSO-S), 44.6 (*C*H_3, DMSO-S), 43.7 (*C*H_3, DMSO-S), 33.7 (C^1H_2+C^2H_2, suc). Selected IR (KBr, cm^{-1}): $\nu_{asym(COO)}$ 1566 (s); $\nu_{sym(COO)}$ 1390 (s); $\nu_{S=O}$ 1094 (s); ν_{Ru-S} 428 (s). UV−vis spectrum (λ_{max}, nm (ϵ, M^{-1} cm^{-1})): 290 (872), 333 (1116).

[K]*fac*-[RuCl(DMSO-S)$_3$(η^2-ox)] (14). A 200 mg amount of **1** (0.412 mmol) was partially dissolved in 1 mL of DMSO. K_2(ox) (68 mg, 0.412 mmol) was added to the stirred mixture that was refluxed for 1 h yielding (after about 10 min) a yellow solution. A white solid (KCl) began to form after 20 min. The mixture was filtered still hot to remove the solid, which was washed with 0.5 mL of DMSO and 3−4 mL of ethanol. Upon standing at room temperature, a pale yellow solid formed and was removed by filtration, washed with cold ethanol and diethyl ether, and vacuum-dried. Yield: 120 mg (59%). Anal. Calcd for $C_8H_{18}ClKO_7RuS_3$ (M_r 498.03): C 19.3, H 3.64. Found: C 18.9, H 3.56. Complex **14** is fairly soluble in water, DMSO, and methanol, slightly soluble in ethanol, DMF, and acetonitrile, and insoluble in acetone, dichloromethane, chloroform, and THF. ^{1}H NMR (D_2O, δ ppm): 3.45 (s, 6H, DMSO-S), 3.43 (s, 6H, DMSO-S), 3.21 (s, 6H, DMSO-S). ^{13}C{^{1}H} NMR (D_2O, δ ppm): 171.3 (*C*OO), 49.2 (*C*H_3, DMSO-S), 47.9 (*C*H_3, DMSO-S), 46.2 (*C*H_3, DMSO-S). Selected IR (KBr, cm^{-1}): $\nu_{asym(COO)}$ 1666 (vs); $\nu_{sym(COO)}$ 1385 (m); $\nu_{S=O}$ 1114 (s); ν_{Ru-S} 427 (m). UV−vis spectrum (λ_{max}, nm (ϵ, M^{-1} cm^{-1})): 289 sh (1606), 350 sh (587).

[{*fac*-RuCl(DMSO-S)$_3$}$_2$(η^4,μ -ox)] (15). K_2(ox) (17 mg, 0.102 mmol) was added to a solution of **1** (100 mg, 0.204 mmol) in water (2 mL). Yellow crystals formed overnight and were removed by filtration, washed with water and acetone, and vacuum-dried at room temperature. Yield: 41 mg (48%). Anal. Calcd for [$C_{14}H_{36}Cl_2O_{10}Ru_2S_6$] ($M_r$ 829.83): C 20.3, H 4.37. Found: C 21.3, H 4.48. Compound **15** is slightly soluble only in water, while it is insoluble in all the other tested solvents (i.e., methanol, ethanol, DMSO, chloroform, acetone, dichloromethane, acetonitrile, DMF, THF, and nitromethane). ^{1}H NMR (D_2O, δ ppm): 3.50 (s, 12H, DMSO-S), 3.48 (s, 12H, DMSO-S), 3.29 (s, 12H, DMSO-S). ^{13}C{^{1}H} NMR (D_2O, δ ppm) (the solubility was barely sufficient for recording the spectrum, but we were unable to observe the *C*OO resonance): 49.72 (DMSO-S), 48.46 (DMSO-S), 47.12 (DMSO-S). Selected IR (KBr, cm^{-1}): $\nu_{asym(COO)}$ 1614 (vs); $\nu_{S=O}$ 1103 (s); ν_{Ru-S} 428 (m). UV−vis spectrum (λ_{max}, nm (ϵ, M^{-1} cm^{-1})): 227 (5852), 298 (872).

***fac*-[Ru(DMSO-S)$_3$(DMSO-O)(η^2-ox)] (16).** A 100 mg amount of **3** (0.115 mmol) was partially dissolved in DMSO (1 mL). K_2(ox) (19 mg, 0.115 mmol) was added, and the stirred mixture was refluxed for 1 h yielding (after about 10 min) a yellow solution. Addition of ethanol (3−4 mL) induced the precipitation of a white solid that was removed by filtration, washed with cold ethanol and diethyl ether, and vacuum-dried at room temperature. Yield: 50 mg (84%). Anal. Calcd for [$C_{10}H_{24}O_8RuS_4$]·H_2O (M_r 519.62): C 23.11, H 5.04. Found: C 22.7, H 4.80. This complex is soluble in water, DMSO, and DMF, slightly soluble in methanol and THF, and insoluble in a number of usual solvents such as ethanol, acetone, dichloromethane, chloroform, acetonitrile, and DMF. ^{1}H NMR (D_2O, δ ppm): 3.42 (s, 6H, DMSO-S), 3.38 (s, 6H, DMSO-S), 3.22 (s, 6H, DMSO-S), 2.81 (s, 6H, DMSO-O). ^{13}C{^{1}H} NMR (D_2O, 278 K, δ ppm): 170.9 (*C*OO), 47.6 (*C*H_3, DMSO-S), 47.2 (*C*H_3, DMSO-S), 46.8 (*C*H_3, DMSO-S), 39.6 (*C*H_3, DMSO-O). Selected IR (KBr, cm^{-1}): $\nu_{asym(COO)}$ 1663 (vs); $\nu_{sym(COO)}$ 1385 (s); $\nu_{S=O}$ (DMSO-S) 1106 (s); $\nu_{S=O}$ (DMSO-O) 933 (m); ν_{Ru-O} 524 (w); ν_{Ru-S} 431 (m). UV−vis spectrum (λ_{max}, nm (ϵ, M^{-1} cm^{-1})): 283 sh (1441), 334 sh (457).

Table 3. Selected Coordination Bond Lengths (Å) and Angles (deg) for Compounds **6**, **7**, **9**, and **10**

	6·2H$_2$O	**7**	**9**·1.5H$_2$O	**10**·H$_2$O
Ru−O(4)		2.138(4)		2.128(3)
Ru−O(5)	2.103(3)	2.087(4)	2.088(3)	2.080(3)
Ru−O(6)	2.097(3)	2.081(4)	2.103(3)	2.074(3)
Ru−S(1)	2.2599(12)	2.2400(17)	2.2614(15)	2.2546(10)
Ru−S(2)	2.2601(11)	2.2513(16)	2.2516(14)	2.2507(11)
Ru−S(3)	2.2487(11)	2.2662(16)	2.2398(15)	2.2707(12)
Ru−Cl(1)	2.4267(14)		2.4316(18)	
O(5)−Ru−O(6)	86.82(12)	88.95(15)	85.90(14)	87.31(11)
O(4)−Ru−S(1)		177.13(12)		176.87(9)
O(5)−Ru−S(3)	176.59(10)	170.70(12)	177.05(12)	171.05(10)
O(6)−Ru−S(2)	178.29(9)	173.54(13)	177.03(10)	173.63(9)
S(1)−Ru−Cl(1)	175.08(4)		176.90(6)	

Table 4. Selected Coordination Bond Lengths (Å) and Angles (deg) for Compounds **8**, **11**, and **13**[a]

	8		**11**·H_2O		
	A	B	A	B	**13**·2EtOH
Ru(1)−O(2)	2.111(2)	2.116(2)	2.107(2)	2.110(3)	2.138(9)
Ru(1)−O(3')	2.106(2)	2.108(2)	2.115(3)	2.112(2)	2.115(9)
Ru(1)−O(1w)	2.144(2)	2.152(2)	2.155(3)	2.143(3)	2.140(10)
Ru(1)−S(1)	2.278(1)	2.274(1)	2.2648(13)	2.2602(12)	2.264(4)
Ru(1)−S(2)	2.255(1)	2.274(1)	2.2415(10)	2.2810(12)	2.246(4)
Ru(1)−S(3)	2.265(1)	2.250(1)	2.2795(12)	2.2461(11)	2.265(4)
Ru(1)−Ru(1')	6.529(2)	6.485(2)	6.428(2)	6.424(2)	6.604(4)
O(2)−Ru(1)−S(2)	178.09(7)	175.94(6)	177.80(8)	176.98(8)	177.2(3)
O(3')−Ru(1)−S(3)	177.31(7)	178.69(7)	176.82(8)	177.15(8)	175.4(3)
O(1w)−Ru(1)−S(1)	170.38(7)	170.44(7)	170.46(8)	171.30(8)	172.8(3)

[a] Primed atoms referred by an inversion center (see figures),

Scheme 2. Reactivity of **1** toward K_2(mal), K_2(mmal), and K_2(dmmal)

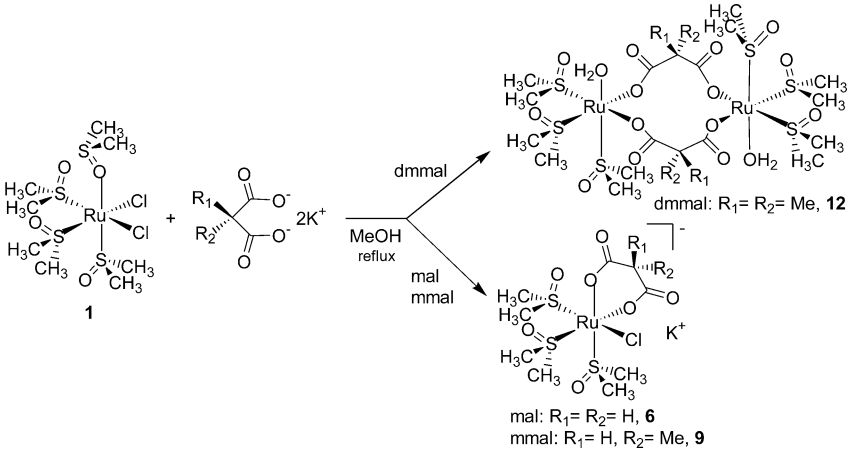

[{*fac*-Ru(DMSO-S)$_3$(DMSO-O)}$_2$(η^4,μ-ox)][CF_3SO_3]$_2$ (17). K_2(ox) (14.25 mg, 0.0865 mmol) was added to a 150 mg amount of **3** (0.173 mmol) partially dissolved in DMSO (1.5 mL). The mixture was refluxed for 1 h yielding a yellow solution. Addition of ethanol (3−4 mL) induced the slow formation (24 h) of a pale yellow microcrystalline solid that was removed by filtration, washed with cold ethanol and diethyl ether, and vacuum-dried at ambient temperature. Yield: 43 mg (41%). Anal. Calcd for [$C_{20}H_{48}F_6O_{18}Ru_2S_{10}$] ($M_r$ 1213.32): C, 19.8; H, 3.99. Found: C, 19.7; H, 4.00. Compound **14** is soluble in water, slightly soluble in DMSO and DMF, and insoluble in methanol, ethanol, acetone, dichloromethane, and chloroform. ^{1}H NMR (D_2O, δ ppm): 3.51 (s, 12H, DMSO-S), 3.44 (s, 12H, DMSO-S), 3.37 (s, 12H, DMSO-S), 2.92 (s, 12H, DMSO-O). ^{13}C{^{1}H} NMR (D_2O, 278 K, δ ppm): 175.8 (*C*OO), 48.0 (*C*H_3, DMSO-S), 47.8 (*C*H_3, DMSO-S), 47.0 (*C*H_3, DMSO-S), 39.6 (*C*H_3, DMSO-O). Selected IR (KBr, cm^{-1}): $\nu_{asym(COO)}$ 1619 (s); $\nu_{S=O}$ (DMSO-S) 1124 (s); $\nu_{S=O}$ (DMSO-O) 925 (m); ν_{Ru-O} 517 (w); ν_{Ru-S} 431 (m). UV−vis spectrum (λ_{max}, nm (ϵ, M^{-1} cm^{-1})): 294 (3686).

[*fac*-Ru(DMSO-S)$_3$(η^3,μ-ox)]$_4$ (18). K_2(ox) (20.8 mg, 0.12 mmol) was added to a warm stirred solution of **3** (87 mg, 0.10 mmol) in methanol (2 mL). The solution was heated to reflux for 48 h. During this time, complex **18** precipitated as a white solid in low yield; it was collected by filtration, washed with cold methanol, and dried in vacuo. Yield 9.2 mg (21%). Additional crystals of **18** suitable for X-ray analysis were obtained from the mother liquor on standing. Anal. Calcd for [$C_{32}H_{72}O_{28}Ru_4S_{12}$] ($M_r$ 1693.97): C, 22.7; H, 4.28. Found: C, 22.5; H, 4.42. This complex is soluble in water, nitromethane, and acetonitrile, slightly soluble in methanol, DMSO, DMF, and acetone, and insoluble in ethanol, dichloromethane, and chloroform. ^{1}H NMR (D_2O, δ ppm): 3.70 (s, 12H, DMSO-S), 3.49 (s, 12H, DMSO-S), 3.45 (s, 12H, DMSO-S), 3.38 (s, 12H, DMSO-S), 3.31 (s, 12H, DMSO-S), 3.22 (s, 12H, DMSO-S). ^{13}C{^{1}H} NMR (D_2O, δ ppm) (the solubility was sufficient for recording the spectrum, but we were unable to observe the *C*OO resonance): 46.3 (*C*H_3, DMSO-S), 46.1 (*C*H_3, DMSO-S), 45.5 (*C*H_3, DMSO-S), 45.1 (*C*H_3, DMSO-S), 44.9 (*C*H_3, DMSO-S), 44.6 (*C*H_3, DMSO-S). Selected IR (KBr, cm^{-1}): $\nu_{asym(COO)}$ 1693 (s), 1671 (s), 1605 (s); $\nu_{sym(COO)}$ 1421 (m); $\nu_{S=O}$ 1111 (s); ν_{Ru-S} 432 (m). UV−vis spectrum (λ_{max}, nm (ϵ, M^{-1} cm^{-1})): 285 sh (7519), 329 sh (2666).

Crystallographic Measurements. Diffraction data for all the reported structures were collected on a Nonius DIP-1030H system (Mo− Kα radiation, λ = 0.71073 Å), except for compound **13**, whose intensity data were measured on a Brucker Kappa CCD imaging plate mounted on a Nonius FR591 rotating anode (Cu− Kα radiation, λ = 1.54178 Å). Cell refinement, indexing, and scaling of the data sets were carried out using the packages Mosflm,[24] Scala,[24] and Denzo.[25] The choice of the noncentrosymmetric space group for **6** and **10** was confirmed by the successful final refinement. The difference Fourier maps of **6**, **9**, **10**, **11**, and **18** revealed some residuals interpreted as water oxygens (some at half occupancy), while a molecule of ethanol (per metal ion) was detected in the crystal of **13**. The disordered molecules of solvent in **13** and the high thermal displacement of triflate atoms in **17** slightly affected the accuracy of the crystal data. All the structures were solved by Patterson and Fourier analyses[26] and refined by the full-matrix least-squares method based on F^2 with all observed

(24) Collaborative Computational Project, No. 4. *Acta Crystallogr., Sect. D* **1994**, *50*, 760−763.

(25) Otwinowski, Z.; Minor, W. In *Processing of X-ray Diffraction Data Collected in Oscillation Mode*; Carter, C. W., Jr., Sweet, R. M., Eds.; Methods in Enzymology, Volume 276: Macromolecular Crystallography, Part A; Academic Press: New York, 1997; Vol 276, pp 307−326.

Table 5. Selected Coordination Bond Lengths (Å) and Angles (deg) for Compounds **15**, **17**, and **18**

		17[a]		
	15	A	B	**18**·5H_2O[b]
Ru−O(4)		2.129(7)	2.128(8)	2.108(5)
Ru−O(5)	2.136(2)	2.119(7)	2.128(8)	2.085(5)
Ru−O(6)	2.142(2)	2.135(7)	2.132(7)	2.087(5)
Ru−S(1)	2.2536(10)	2.228(3)	2.229(3)	2.259(2)
Ru−S(2)	2.2421(10)	2.259(3)	2.242(4)	2.257(2)
Ru−S(3)	2.2916(10)	2.263(4)	2.262(4)	2.256(2)
Ru−Cl(1)	2.4192(11)			
Ru−Ru′	5.501(2)	5.523(2)	5.517(3)	5.608(1)
O(5)−Ru−O(6)	78.53(8)	78.9(3)	79.2(3)	79.62(19)
O(5)−Ru−S(2)	173.43(6)	172.5(2)	172.0(2)	172.17(14)
O(6)−Ru−S(1)	167.82(6)	171.2(2)	172.5(2)	171.60(15)
O(4)−Ru(1)−S(3)		175.8(2)	176.3(2)	174.70(16)
S(3)−Ru−Cl(1)	171.34(3)			

[a] Ru═Ru(1); see Figure 6. [b] O(4)═O(4″) at $y - 1/4$, $-x + 5/4$, $-z + 1/4$; see Figure 7.

Chart 2

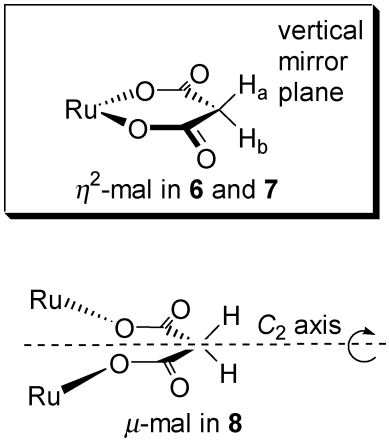

reflections.[26] All the calculations were performed using the WinGX System, version 1.70.01.[27] Crystal data and details of refinements are reported in Tables 1 and 2, and a selection of bond lengths and angles is shown in Tables 3−5.

Results

Malonato (mal), Methylmalonato (mmal), and Dimethylmalonato (dmmal) Complexes. Treatment of *cis*,*fac*-[$RuCl_2$(DMSO-S)$_3$(DMSO-O)] (**1**) with 1 equiv of the potassium salt of malonate, K_2(mal), in refluxing methanol afforded, upon slow evaporation of the solvent (i.e., under the same conditions that with cbdc led to the dinuclear species **4**), the mononuclear anionic species [K]*fac*-[RuCl(DMSO-S)$_3$(η^2-mal)] (**6**) (Scheme 2), similar to the cbdc complex **5**.[16] The same product was obtained using *trans*-[$RuCl_2$(DMSO-S)$_4$] (**2**) as a starting material.

Compound **6** was characterized also by X-ray structural analysis (Figure 1, Table 3, and Supporting Information). In **6**, the metal displays the expected distorted octahedral geometry, and the coordination sphere is comprised of one malonate acting as chelating ligand through the two carboxylic groups, of three DMSO-S ligands in facial geometry, and one chloride. The malonate presents the usual bidentate coordination mode (η^2, chelating angle of 86.82(12)°), with a twist-boat conformation. The Ru−O bond lengths are comparable within their esd values, and the Ru−S and Ru−Cl bond lengths are typical of Ru(II)-chloride-DMSO complexes.[28] In the solid state, the K^+ counterion acts as a bridge between two adjacent complexes through ionic interactions with the Cl^- of one unit and the three DMSO oxygens of the other, thus producing 1-D polymeric chains (Supporting Information); in addition, K^+ completes the coordination sphere with two lattice water molecules.

In the IR spectrum, there are two bands for the chelating malonate, at 1575 and 1414 cm^{-1}, attributed to the asym-

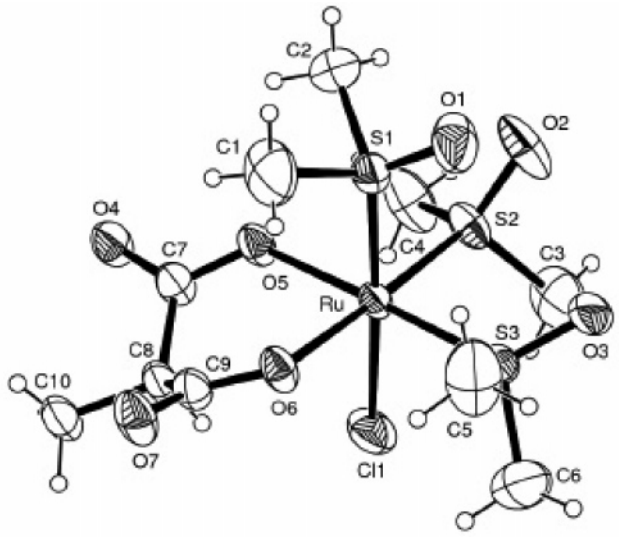

Figure 1. Molecular structure of the complex anion of [K]*fac*-[RuCl(DMSO-S)$_3$(η^2-mmal)]·1.5H_2O (**9**) (thermal ellipsoids at 40% probability level) and labeling scheme for the non-hydrogen atoms. The same drawing applies also to the corresponding mal complex **6**, with an H in place of C10.

Table 6. ^{13}C NMR Chemical Shifts (D_2O) and Carboxylate Stretching Frequencies for Compounds **4**−**19**

compound (dicarb ligand and its coordination mode)	^{13}C (*C*OO), δ	^{13}C (C^1), δ	$\nu_{asym(COO)}$	$\nu_{sym(COO)}$
4 (μ-cbdc)	188.3	61.8	1586	1387, 1361
19 (μ-cbdc)	186.5	61.9	1599	1379, 1356
5 (η^2-cbdc)	188.1	57.5	1604	1383
6 (η^2-mal)	181.6	47.6	1575	1414
6a (η^2-mal)	180.8	47.4		
7 (η^2-mal)	181.4	48.2	1613	1375
8 (μ-mal)	183.8	52.6	1582	1360
9 (η^2-mmal)	181.6	49.1	1610, 1587	1413
10 (η^2-mmal)	n.d.	n.d.	1608, 1592	1396
11 (μ-dmmal)	186.8	54.7	1586	1408
12 (η^2-dmmal)	187.2	53.1	1581, 1562, 1538	1411
12a (η^2-dmmal)	185.6	52.9		
13 (μ-suc)	188.1	33.7[a]	1566	1390
14 (η^2-ox)	171.3		1666	1385
14a (η^2-ox)	170.6			
15 (η^4,μ-ox)	*b*		1614	
16 (η^2-ox)	170.9		1663	1385
17 (η^4,μ-ox)	175.8		1619	
18 (η^3,μ-ox)	*b*		1693, 1671, 1605	1421

[a] Equivalent C^1 and C^2. [b] Insufficient water solubility.

(26) Sheldrick, G. M. *SHELX97, Programs for Crystal Structure Analysis (Release 97-2)*; University of Göttingen: Göttingen, Germany, 1998.
(27) Farrugia, L. J. *J. Appl. Crystallogr.* **1999**, *32*, 837−838.
(28) (a) Calligaris, M.; Carugo, O. *Coord. Chem. Rev.* **1996**, *153*, 83−154. (b) Calligaris, M. *Coord. Chem. Rev.* **2004**, *248*, 351−375.

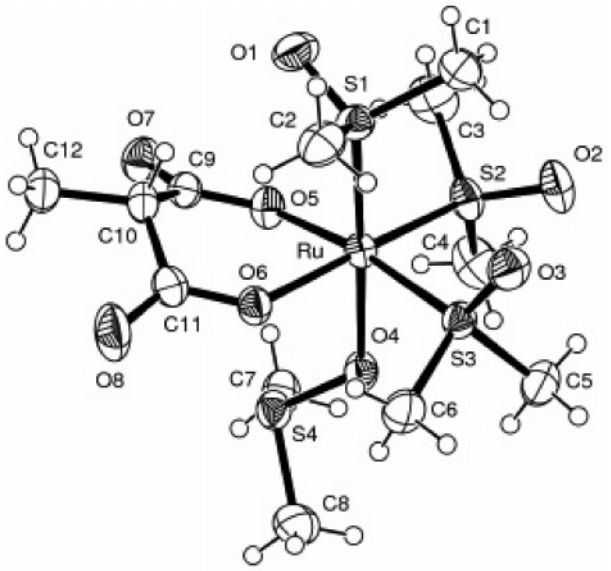

Figure 2. Molecular structure of *fac*-[Ru(DMSO-S)$_3$(DMSO-O)(η^2-mmal)]·H$_2$O (**10**) (thermal ellipsoids at 40% probability level) and labeling scheme for the non-hydrogen atoms. The same drawing applies also to the corresponding mal complex **7**, with an H in place of C12.

metric ($\nu_{asym(COO)}$) and symmetric ($\nu_{sym(COO)}$) carboxylate stretching modes, respectively (Table 6).

The ^{1}H NMR spectrum of complex **6** in D_2O displays three equally intense singlets (6H) in the region of S-bonded DMSO (δ = 3.42, 3.38, 3.21).[29] The sharpest and most upfield DMSO resonance is attributed to the two equivalent methyl groups of the DMSO-S trans to Cl, while the other two pertain to the diastereotopic methyl groups of the two equivalent DMSO-S ligands trans to the carboxylate groups and are slightly broadened by the long-range coupling.[30] This type of pattern for the DMSO methyl resonances is typical for the *fac*-Ru(DMSO-S)$_3$ fragment in *fac*-[Ru(DMSO-S)$_3$-(X)$_2$(Y)] complexes (X, Y = neutral or anionic ligands)[13] and will not be commented on further for the following compounds. Thus, more detailed information about the nature of the species under investigation must be found in the ^{1}H and ^{13}C resonances of the dicarboxylate. In the NMR spectrum of **6**, the malonato ligand has two doublets (1H), at δ = 3.14 and 4.00, for the two diastereotopic methylene protons (Chart 2) that in the 2-D HMQC spectrum are coupled to the same carbon resonance (Supporting Information).

Treatment of *fac*-[Ru(DMSO-S)$_3$(DMSO-O)$_3$][CF$_3$SO$_3$]$_2$ (**3**) with 1 equiv of K$_2$(mal) in refluxing DMSO/methanol mixtures yielded the mononuclear neutral complex *fac*-[Ru-(DMSO-S)$_3$(DMSO-O)(η^2-mal)] (**7**).[31] Crystallization from acetone afforded the complex as colorless crystals, suitable for X-ray analysis (Figure 2, Table 3, and Supporting Information). The coordination sphere of Ru in complex **7** is similar to that of **6** (a chelating malonate and three DMSO-S ligands in facial configuration) except for the O-bonded DMSO that formally replaces the chloride of **6**. The Ru−O(mal) bond lengths (2.081(4) and 2.087(4) Å) are shorter than those found in **6** (2.097(3) and 2.103(3) Å), probably because of the different charge of the two complexes, and the Ru−O(DMSO) bond length (2.138(4) Å) is significantly longer than the Ru−O(mal) distances. The malonate ring adopts a flattened boat conformation.

The ^{1}H NMR spectrum of complex **7** in D_2O is consistent with the molecular structure found in the solid state. The equivalent DMSO-O methyls give a singlet in the region typical for O-bonded DMSO (δ = 2.84), while the diastereotopic protons of the chelating malonate ligand resonate as two doublets at δ = 3.42 and 3.85 ppm, integrating for one proton each and coupled to the same C^1 carbon resonance in the 2-D HMQC spectrum (Supporting Information).

Replacement of K$_2$(mal) with K$_2$(mmal) led, under similar reaction conditions, to the methylmalonato mononuclear species [K]*fac*-[RuCl(DMSO-S)$_3$(η^2-mmal)] (**9**) and *fac*-[Ru-(DMSO-S)$_3$(DMSO-O)(η^2-mmal)] (**10**). The X-ray structural determinations of **9** and **10** (Figures 1 and 2 and Table 3) show that bond distances and angles are very similar to those found in the closely related mal derivatives **6** and **7**, respectively. In both complexes, the chelating dicarboxylate adopts a flattened boat conformation with the H atom on the C^1 in axial position that points toward the chlorine in **9** and toward the S-coordinated DMSO in **10**. Very likely, these are the most stable among the possible isomers.[32] The crystal packing of **9**, unlike that of **6**, consists of a 2-D layered arrangement parallel to the *ac* plane (Supporting Information) obtained through six octahedral K···O ionic interactions (three oxygen atoms from the DMSO-Ss, two from mmal, and one from a lattice water molecule).

On the contrary, the reaction of **1** with K$_2$(dmmal), under the same reaction conditions, led exclusively to isolation of the dinuclear species with two bridging dicarboxylates [*fac*-Ru(DMSO-S)$_3$(H$_2$O)(μ-dmmal)]$_2$ (**11**), similar to **4** (Scheme 2).[33] The corresponding species with mal, [*fac*-Ru(DMSO-S)$_3$(H$_2$O)(μ-mal)]$_2$ (**8**), could be obtained in low yield by treatment of **1** with 1 equiv of Ag$_2$(mal) in dichloromethane at ambient temperature. The structural features of the two independent crystallographic units (A and B) of **8** and of **11** (Figure 3, Table 4, and Supporting Information) closely resemble those of **4**, with a slight difference in the intermetallic distances. In **8**, these are 6.529(2) (A) and 6.485(2) Å (B) that average to the value found in **4**, 6.498(2) Å, while shorter values (6.424(2) and 6.428(2) Å) were measured in **11**. This is a consequence of the narrower C(7)−C(8)−C(9)

(29) The NMR spectra of the new compounds were investigated primarily in D_2O. As all complexes experience hydrolytic processes in aqueous solution, the ^{1}H NMR spectra in D_2O described in this section pertain to fresh solutions exclusively.

(30) Barnes, J. R.; Goggin, P. L.; Goodfellow, R. J. *J. Chem. Res.* **1979**, 1610−1656.

(31) With K$_2$(cbdc), this synthetic procedure led to the dinuclear compound **4**.

(32) In principle, each complex can exist as two stereoisomers that can be formally interconverted by 180° rotation of the chelating mmal (Supporting Information). For both **9** and **10**, only one stereoisomer, presumably the most stable one, was found in the solid state X-ray structures.

(33) As found with cbdc, the mononuclear compound with a chelating dmmal, [K]*fac*-[RuCl(DMSO-S)$_3$(η^2-dmmal)] (**12**), could be isolated as an intermediate in the synthesis of **11**. Similarly to **5**, in aqueous solution, compound **12** slowly evolves to the more stable dinuclear species **11**.

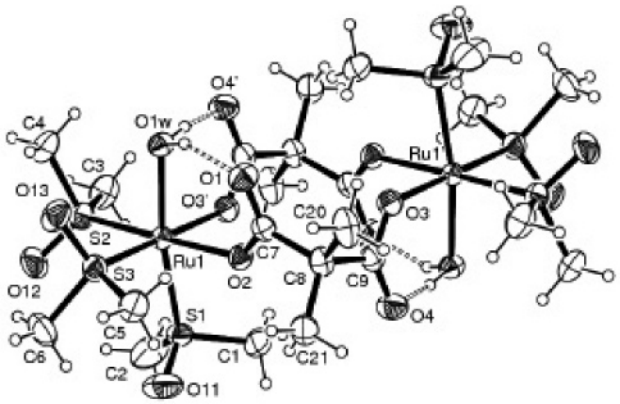

Figure 3. Molecular structure of one of the two independent dinuclear complexes [*fac*-Ru(DMSO-S)$_3$(H$_2$O)(μ-dmmal)]$_2$·H$_2$O (**11**) (thermal ellipsoids at 40% probability level) located on an inversion center. Intramolecular hydrogen bonds are represented with dotted lines.

Scheme 3. Reactivity of **1** toward K$_2$(suc)

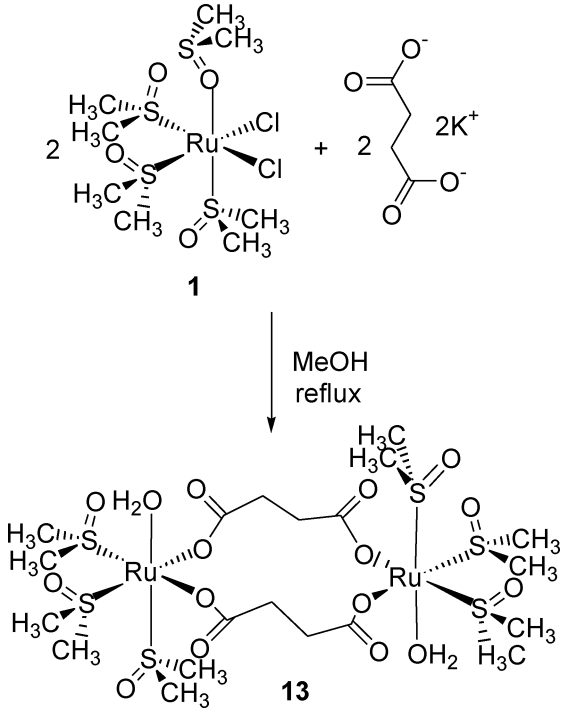

angle in **11** (ca. 105°) due to the steric compression exherted by the dmmal methyl groups. In both compounds, the two coordinated water molecules have an anti geometry, and each of them is involved in two hydrogen bonds with the noncoordinated oxygen atoms of the bridging ligands. The H$_2$O···O distances of the H-bonds fall in the range of 2.581(4) to 2.638(4) Å (in **8**) and 2.595(4) to 2.636(4) Å (in **11**), consistent with strong H-bonds.[15,16]

The ^{1}H NMR spectra of compounds **8** and **11** in D$_2$O are consistent with their dimeric structure and C_i symmetry. In fact, in **8**, the enantiotopic protons of the equivalent malonato ligands (Chart 2) give a singlet that partially overlaps with the DMSO-S resonance at $\delta = 3.34$; this peak is clearly correlated to the malonato C^1 carbon resonance in the 2-D HMQC spectrum (Supporting Information). Similar considerations apply to the ^{1}H NMR (D$_2$O) spectrum of **11**, in which the equivalent methyl groups of the symmetry related dmmal units also give a singlet ($\delta = 1.39$).

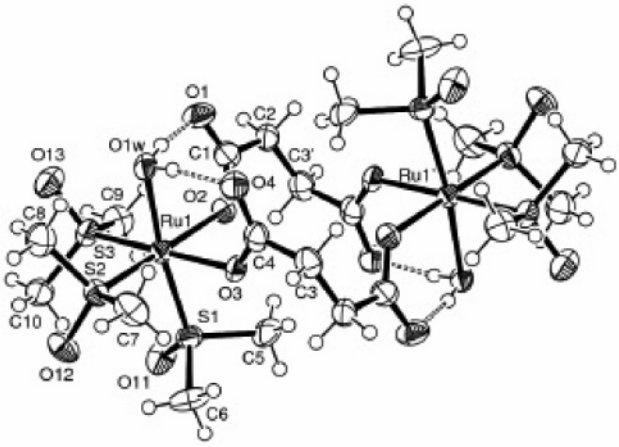

Figure 4. Molecular structure of [*fac*-Ru(DMSO-S)$_3$(H$_2$O)(μ-suc)]$_2$·2EtOH (**13**) (thermal ellipsoids at 40% probability level) and atom labeling scheme for the independent unit. Intramolecular hydrogen bonds are represented with dotted lines.

While the ^{13}C resonance of the two equivalent *C*OO groups in **6**−**12** seems to be mildly influenced by the coordination mode of the dicarboxylate, a trend is apparently found in the resonance of the pivotal carbon atom C^1, which is consistently shifted upfield of ca. 2−4 ppm in the η^2 compounds respective to the μ compounds (Table 6). A similar behavior was found for the C^1 resonance of the cbdc complexes.[16]

Succinato (suc) Complexes. Treatment of **1** with K$_2$(suc) in refluxing methanol yielded the dinuclear compound [*fac*-Ru(DMSO-S)$_3$(H$_2$O)(μ-suc)]$_2$ (**13**) (similar to **4**, **8**, and **11**) in reasonable yield (Scheme 3). We had no evidence of the formation of other species.

The ^{1}H NMR spectrum of **13** is consistent with the C_i symmetry of the complex (C_2 axis bisecting the C^1−C^2 bond of suc): the two equivalent carbon atoms of the equivalent ligands bear pairs of diastereotopic protons, whose resonances (doublets at $\delta = 2.75$ and 2.56) have cross-peaks with the same carbon peak ($C^1 + C^2$) in the 2-D HMQC spectrum (Supporting Information). The X-ray structure obtained for **13** confirmed the centrosymmetric dinuclear nature of the complex, with the two water molecules in anti geometry (Figure 4). The metals are separated by 6.604(4) Å due to the twisted conformation of the C atom backbone in the bridging succinates (torsion angle of 73(1)°). Although the geometrical parameters of **13** are of lower accuracy with respect to the other structures reported, the coordination distances are similar to those observed for **8** and **11** (Table 4). The H-bonding scheme involving the axial water molecules shows O(1w)···O(1) and O(1w)···O(4) distances of 2.574(17) and 2.585(16) Å, respectively.

Oxalato (ox) Complexes. Treatment of either **1** or its isomer **2** with 1 equiv of the potassium salt of oxalate, K$_2$(ox), in warm DMSO yielded the mononuclear anionic complex [K]*fac*-[RuCl(DMSO-S)$_3$(η^2-ox)] (**14**), similar to **5** and **6** (Scheme 4). The ^{1}H NMR spectrum of **14** (three singlets at $\delta = 3.45$, 3.43, 3.21) shows the presence of the

Scheme 4. Reactivity of **1** and **2** toward K_2(ox) in DMSO

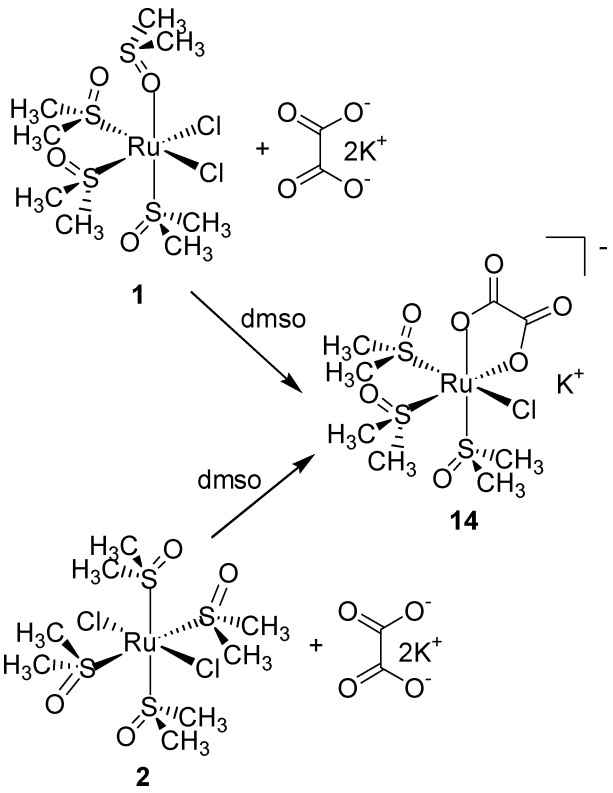

Scheme 5. Reactivity of **1** toward K_2(ox) in Water

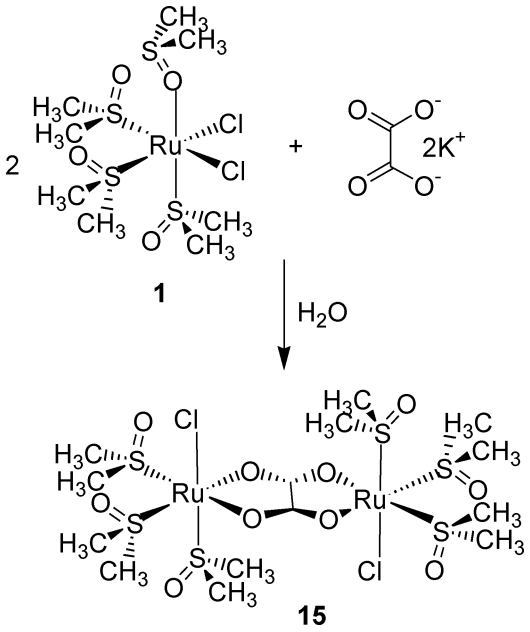

fac-Ru(DMSO-S)$_3$ fragment. Both the IR (asymmetrical and symmetrical COO stretching bands separated by ca. 300 cm^{-1}) and the ^{13}C NMR spectra (a single resonance at δ = 171.3 indicative of two equivalent C atoms) are consistent with a symmetrical bidentate coordination mode for the oxalate in **14** (Table 6).

When **1** was treated with 0.5 equiv of K_2(ox) in aqueous solution (Scheme 5), the dinuclear neutral complex [{*fac*-RuCl(DMSO-S)$_3$}$_2$(η^4,μ-ox)] (**15**) precipitated as yellow crystals suitable for X-ray analysis. The same product had been serendipitously obtained (and characterized only by X-ray crystallography) by Hall and co-workers by treatment of **1** in water with methylsquarate (that decomposed to yield the oxalate ion).[17]

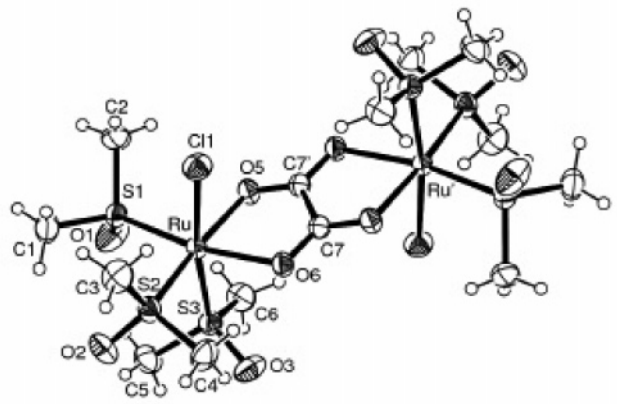

Figure 5. Molecular structure of [{*fac*-RuCl(DMSO-S)$_3$}$_2$(η^4,μ-ox)] (**15**) (thermal ellipsoids at 40% probability level) with labeling scheme for the crystallographically independent unit.

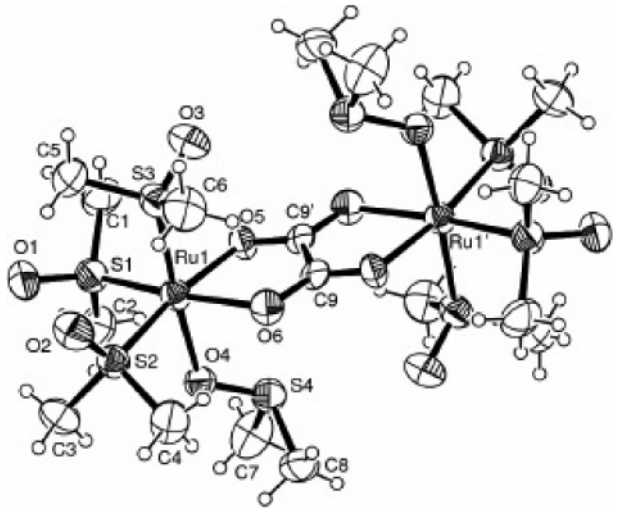

Figure 6. Molecular structure of one of the two independent cations of [{*fac*-Ru(DMSO-S)$_3$(DMSO-O)}$_2$(η^4,μ-ox)](CF$_3$SO$_3$)$_2$ (**17**) (thermal ellipsoids at 40% probability level) with atom labeling scheme for the crystallographically independent unit.

In **15** (Figure 5), the oxalate behaves as a bis-bidentate bridging ligand (the most common coordination mode for this anion) between two *fac*-RuCl(DMSO-S)$_3$ fragments, with an intermetallic distance of 5.501(2) Å. The two chlorides present an anti geometry (the complex is centrosymmetric), and no evidence for the syn isomer was found, both in solution and in the solid state. The coordination bond angles exhibit marked distortions from the ideal geometry (Table 5), to be attributed to the crowding about the metal sphere. In fact, the oxalate forms an angle of 14.7(1)° with the equatorial S_2O_2 mean planes, forcing the chloro ligands to point toward the center of the molecule. The metal is displaced by 0.39 Å from the strictly coplanar oxalate unit.

The reaction of the chloride-free precursor *fac*-[Ru(DMSO-S)$_3$(DMSO-O)$_3$][CF$_3$SO$_3$]$_2$ (**3**) with 1 equiv of K_2(ox) in warm DMSO afforded the mononuclear neutral species *fac*-[Ru(DMSO-S)$_3$(DMSO-O)(η^2-ox)] (**16**), similar to **7** (Scheme 6).

Scheme 6. Reactivity of **3** toward K_2(ox) in DMSO

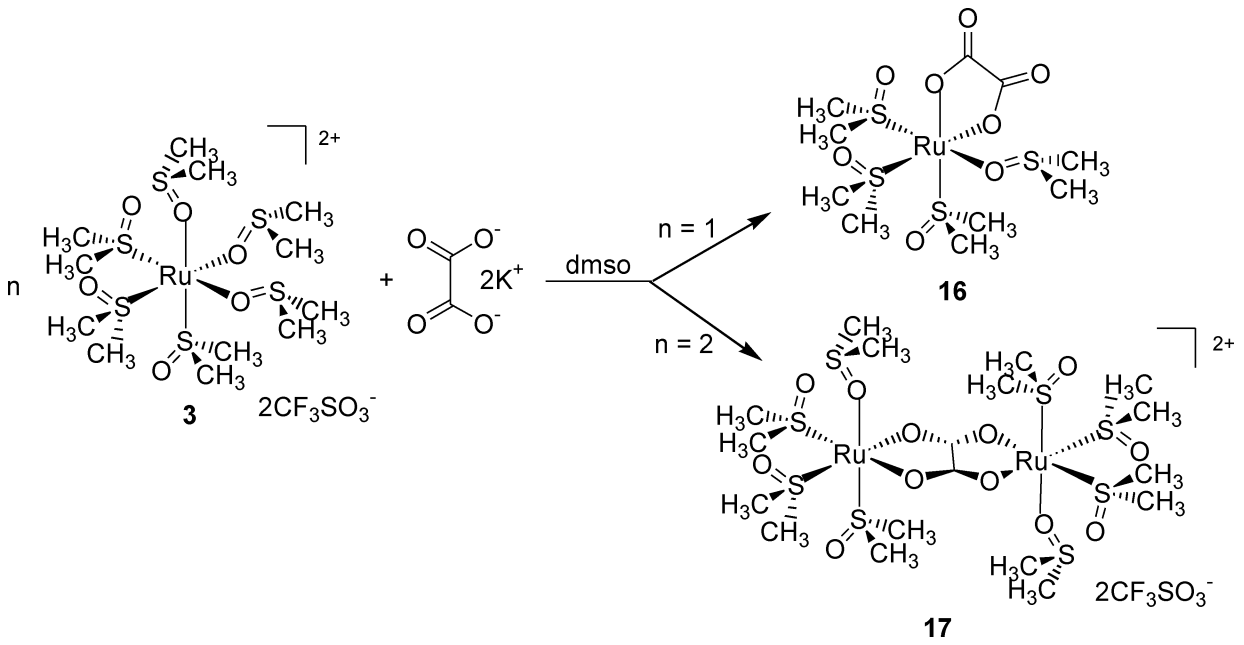

The ^{1}H NMR spectrum of **16** is similar to that of **14**, with the additional singlet (6H) in the DMSO-O region, $\delta = 2.81$. Moreover, treatment of **3** with 0.5 equiv of K_2(ox) afforded the dinuclear cationic species [{*fac*-Ru(DMSO-S)$_3$(DMSO-O)}$_2$(η^4,μ-ox)][CF_3SO_3]$_2$ (**17**) (Scheme 6), which is similar to **15**, with DMSO-O ligands formally replacing the two chlorides. The nature of **17** was confirmed by the X-ray structural analysis (Figure 6), which evidenced two crystallographic independent cations in the unit cell, both arranged about an inversion center. Also in this case the anti geometrical isomer was selectively obtained. The geometries of the two independent cations are closely comparable. The oxalate is coplanar with the equatorial S_2O_2 mean planes, and the Ru···Ru distances in the two molecules are 5.523(2) and 5.517(3) Å, slightly longer than in **15**, likely due to the bulkier DMSO-O ligands.

The ^{1}H NMR spectra of **15** and **17** in D_2O (**15** is sparingly soluble) display the typical pattern for the three DMSO-S ligands in facial geometry, while the occurrence of only one COO stretching absorption in the IR spectra (Table 6) is consistent with the bis-bidentate bridging binding mode of oxalate.

Finally, we found that prolonged heating of **3** with a slight excess of K_2(ox) in refluxing methanol afforded the neutral tetranuclear complex [*fac*-Ru(DMSO-S)$_3$(η^3,μ-ox)]$_4$ (**18**) as colorless square plates (Scheme 7). For shorter reaction times, a mixture of compounds **17** and **18** was obtained, suggesting that **17** is an intermediate in the synthesis of **18**.

The molecular structure of **18** is shown in Figure 7, with selected bond lengths and angles given in Table 5. The metallacycle (or molecular square) is built up by the oxalate anions that bridge two neighboring Ru atoms in an unsymmetrical manner: one side of each oxalate unit acts as a chelate through O4 and O5, while the other side binds a neighboring ruthenium through O(6). The Ru−O(4) and Ru−O(5) distances (2.085(5) and 2.087(5) Å, respectively) are

Scheme 7. Reactivity of **3** toward K_2(ox) in Refluxing MeOH

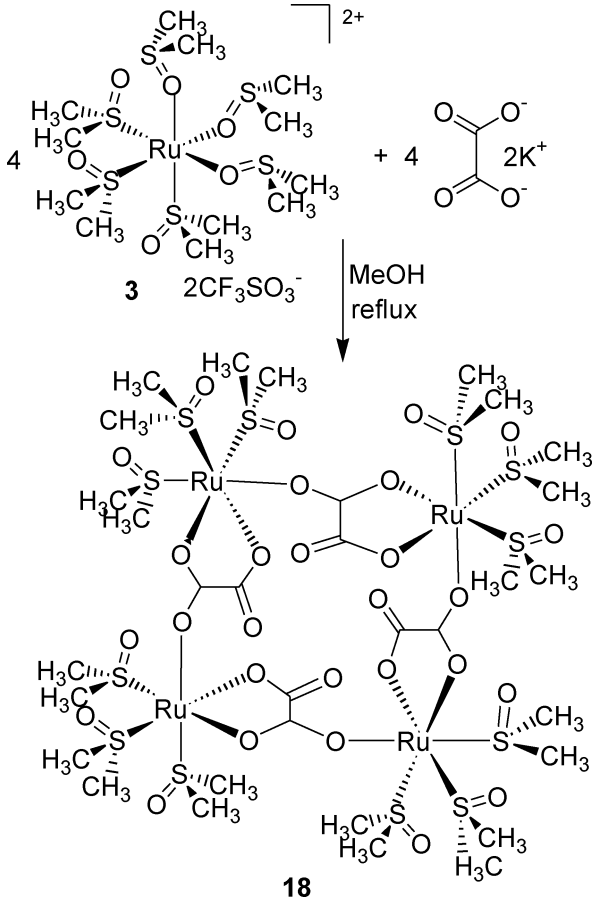

slightly shorter than the Ru−O(6′) distance (2.108(5) Å, involving an oxygen from a symmetry related oxalate). The Ru(oxalate) units are related by a S_4 inversion axis with an intermetallic distance of 5.608(1) Å. The symmetry axis induces a non-coplanar setting of the four Ru atoms that are alternatively located at 0.784(1) Å above and below their mean plane. Each oxalate fragment forms a dihedral angle

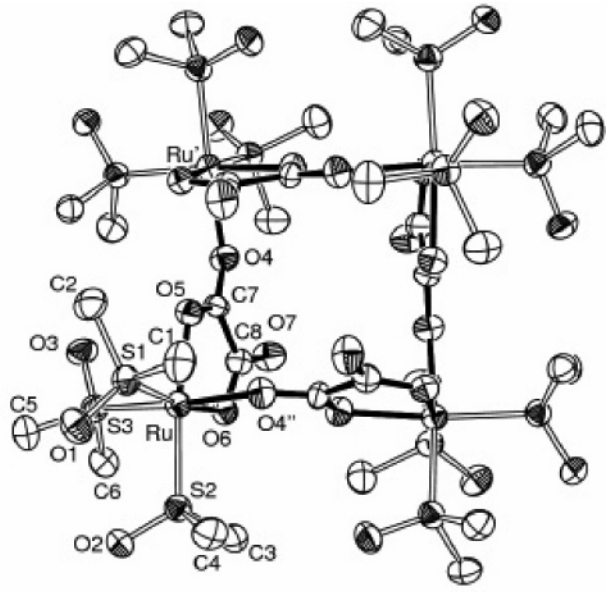

Figure 7. Molecular structure of the tetranuclear species of [*fac*-Ru(DMSO-S)$_3$(η^3,μ-ox)]$_4$·5H$_2$O (**18**) with atom labeling scheme of the crystallographically independent part.

of 72.3(1)° with the mean plane through the metals, with oxygens O(7), not involved in coordination, that point alternatively on opposite sides of the Ru$_4$ plane. This feature considerably reduces the expected void inside the tetranuclear compound (Supporting Information). Each Ru center completes the distorted octahedral coordination sphere with three DMSO-S molecules in facial position. The crystal structure reveals the presence of lattice water molecules (5 per tetranuclear unit) that are H-bonded to form a 1-D chain filling void channels between the metallacycles along axis *a* (and along *b* for symmetry) (Supporting Information).

The ^{1}H NMR spectrum of **18** in D$_2$O exhibits six equally intense singlets in the region for S-bonded DMSO and is consistent with the cyclic tetranuclear structure found in the solid state. In fact, even though all four Ru fragments are related by symmetry, the three DMSO-S ligands on each metal center are inequivalent, and each of them has diastereotopic methyl groups. In the IR spectrum of **18**, four bands are observed for the oxalate ligand (Table 6).

Even though the crystals of **18** obtained from methanol are relatively well-soluble in water, from the concentrated D$_2$O solutions used for NMR studies we observed the formation, within a few days, of colorless crystals. X-ray structural investigation showed that such crystals contain the same compound **18** with a slightly different orientation of the oxalate mean planes and, interestingly, without any lattice water molecule (Supporting Information).

Chemical Behavior in Aqueous Solution. The behavior of selected compounds in aqueous solution was investigated by NMR spectroscopy at room temperature in pure D$_2$O and in 100 mM NaCl solutions (for mimicking the extracellular chloride concentration found in plasma). The effect of the addition of 100 mM NaCl on the equilibrium established in D$_2$O between each compound and its hydrolyzed species was studied as well.

Scheme 8. Chemical Behavior of Compounds **6** and **7** in Aqueous Solution

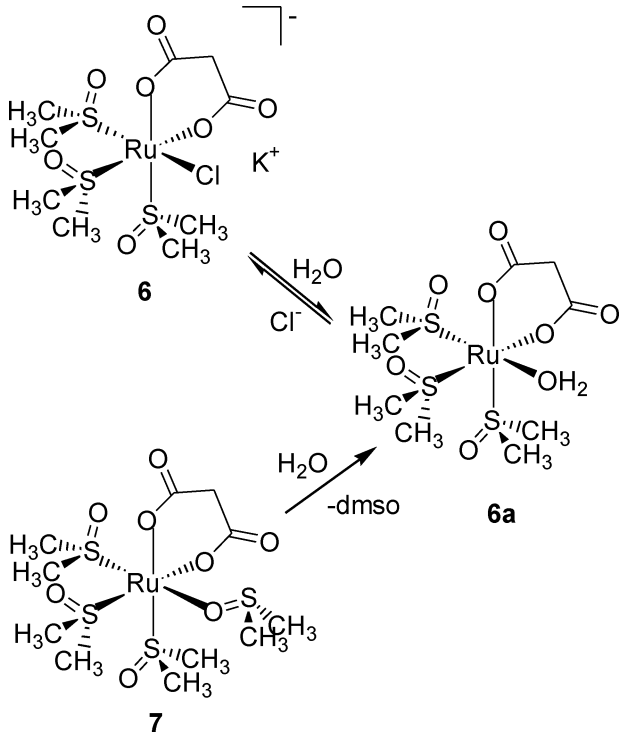

The ^{1}H NMR spectrum of complex **6** in D$_2$O changed slowly with time (days): the three DMSO-S resonances of **6** were gradually replaced by three new equally intense singlets in the same region (at δ = 3.23, 3.37, 3.42),[34] attributed to an aquated species **6a**. No signals for free DMSO or malonate were observed (both in ^{1}H and ^{13}C NMR spectra). However, the two doublets arising from the malonate protons of **6** disappeared slowly with time, without the appearance of any new resonance. This behavior was attributed to a slow exchange of the slightly acidic CH$_2$ protons of coordinated malonate with deuterium and was confirmed by monitoring the hydrolysis of **6** by ^{1}H NMR in a H$_2$O/D$_2$O (9:1) mixture, in which the exchangeable protons can be detected. In this experiment, the decrease of the malonate doublets of **6** was accompanied by the appearance of two new doublets for **6a** (at δ = 3.59 and 3.29, coupled to each other in the ^{1}H−^{1}H COSY spectrum), which are coupled to the *C*^{1} resonance (Table 6) in the HMQC spectrum (Supporting Information).[35] According to the previous experimental evidence, it can be deduced that, once dissolved in water, complex **6** slowly releases the Cl$^-$ anion yielding the aquo complex *fac*-[Ru(DMSO-S)$_3$(H$_2$O)(η^2-mal)] (**6a**) (Scheme 8). After 7 days, the ratio between **6** and **6a** was ca. 1:2 and remained unchanged afterward. The addition of

(34) The resonance at δ = 3.42 overlaps with a resonance from **6**. This is evident in the HMQC spectrum, in which this singlet has cross-peaks with two well-separated signals in the carbon dimension (Supporting Information).

(35) The ^{13}C{^{1}H} NMR spectrum of **6a** consists of three resonances close to each other in the DMSO region (at δ = 46.6, 46.7, and 46.7), one resonance for the malonate CH$_2$ at δ = 47.4, and one resonance for the two equivalent carboxylates at δ = 180.8. Thus, the ^{13}C NMR spectrum confirms that the malonate ligand remains coordinated to Ru in **6a** since no signals of the free ligand (at δ = 179.7 and 49.5) were observed.

Scheme 9. Chemical Behavior of the Dinuclear Compound **8** in Aqueous Solution

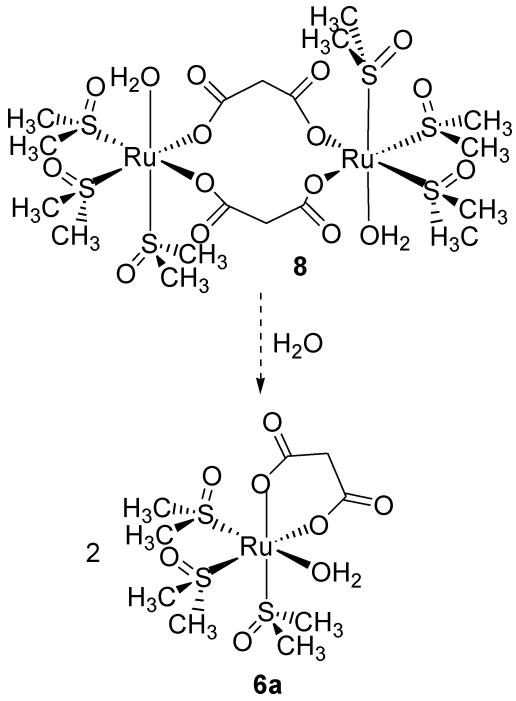

100 mM NaCl in the previous solution reverted the ratio between **6** and **6a** from 1:2 to 4:1 (within 48 h). Similarly, the hydrolysis of **6** proceeded only to ca. 20% in the presence of 100 mM Cl^-.

A remarkably similar behavior in aqueous solution was observed for *fac*-[Ru(DMSO-S)$_3$(DMSO-O)(η^2-mal)] (**7**) (Scheme 8). The hydrolytic process involves the complete release, within ca. 2 h, of the O-bonded DMSO molecule, as indicated by the decrease of the resonance at $\delta = 2.84$ and the simultaneous increase of the resonance of free DMSO at $\delta = 2.71$. At the same time, the other resonances of **7** were gradually replaced by those of **6a**. Addition of 100 mM NaCl to the equilibrated D_2O solution induced the slow formation of **6**; an equilibrium ratio of 1:4 between **6a** and **6** was reached after 6 days and remained unchanged afterward. The same equilibrium mixture was obtained when the hydrolysis of **7** was performed in the presence of 100 mM NaCl (Scheme 8). The mmal species **9** and **10** behave in aqueous solutions similarly to the corresponding mal compounds.

NMR spectroscopy (^{1}H and ^{13}C) showed that, similarly to **6** and **7**, also dimer **8** upon dissolution in D_2O slowly yields *fac*-[Ru(DMSO-S)$_3$(H$_2$O)(η^2-mal)] (**6a**) as main product (Scheme 9).

Remarkably, this behavior is opposite to what observed with cbdc and dmmal species. The hydrolytic process was complete in ca. 5 days and involved unidentified intermediate species characterized by DMSO-S resonances (minor DMSO dissociation was also observed). In fact, while the hydrolysis of **6** and **7** to **6a** is a one-step process, the formation of **6a** from **8** is a multi-step process, involving a change in the coordination mode of the malonate units from bridging (μ, in **8**) to chelating (η^2 in **6a**). Addition of 100 mM NaCl to the equilibrated solution caused, within ca. 5 days, the settlement of an equilibrium between **6a** and **6**, in a ratio of 1:4. The same equilibrium was observed within 3 days, when the hydrolytic process was performed in 100 mM NaCl solution.

The chemical behavior of the dimethylmalonato complexes **11** and **12** is similar to that of the corresponding cbdc analogues, **4** and **5**. Dimer **11** is very stable in aqueous solutions. Monomer **12** initially undergoes partial hydrolysis of Cl^-, yielding within 1 day the aquo species *fac*-[Ru(DMSO-S)$_3$(H$_2$O)(η^2-dmmal)] (**12a**). This process is followed by the formation of **11** (after 1 week, this species is predominant in the solution), indicating that the dimer is the thermodynamically stable product.

Similar to the cbdc (**4**) and dmmal (**11**) dimers, and contrary to **8**, the succinate dimer **13** is also very stable in aqueous solutions. No significant spectral changes were observed over a 2 week period.

The chemical behavior of the mononuclear oxalato species **14** and **16** is similar to those of the corresponding malonato complexes **6** and **7**. Upon dissolution in D_2O, the DMSO-S resonances of [K]*fac*-[RuCl(DMSO-S)$_3$(η^2-ox)] (**14**) were slowly replaced by three new equally intense singlets (two of which overlap with those of **14**), and no signal for free DMSO was observed. After 2 weeks, the system reached the equilibrium, with a ratio 1:2 between **14** and the new species **14a.** The DMSO-S singlets of **14a** ($\delta = 3.45$, 3.41, 3.21) were also observed to grow when the neutral compound *fac*-[Ru(DMSO-S)$_3$(DMSO-O)(η^2-ox)] (**16**) was dissolved in water. The complete hydrolysis of the O-bonded DMSO occurred within 2 h, and no further changes were observed in the NMR spectrum afterward (3 weeks). Thus, the new species **14a** was unambiguously identified as the aquo compound *fac*-[Ru(DMSO-S)$_3$(H$_2$O)(η^2-ox)]. The single ^{13}C NMR resonance observed for the coordinated oxalate in **14a** ($\delta = 170.6$) confirms the symmetrical coordination of the dianion. When the hydrolysis of either **14** or **16** was performed in 100 mM NaCl solution, an equilibrium mixture of 3:1 between **14** and **14a** was reached within ca. 1 week. The same results were obtained by addition of 100 mM NaCl to the equilibrated aqueous solutions.

The cationic dinuclear compound [{*fac*-Ru(DMSO-S)$_3$-(DMSO-O)}$_2$(η^4,μ-ox)]$^{2+}$ (**17**) is unstable in aqueous solution. Within a few hours after dissolution in D_2O, several new signals appeared both in the region of S-bonded and in that of O-bonded DMSO in the ^{1}H NMR spectrum, together with the signal of free DMSO. After 2 weeks, two main species were present in solution: compound **14a** and another species **14b**, characterized by a singlet at $\delta = 3.44$ for ca. three equivalent DMSO-S ligands (owing to the presence of other minor species, integration was not particularly accurate). According to integration, the peak of free DMSO corresponds ca. to two molecules (i.e., the two original dsmo-O ligands). Thus, after dissolution in water, compound **17** undergoes the stepwise hydrolysis of the two O-bonded DMSO ligands yielding the monoaquo [{*fac*-Ru(DMSO-S)$_3$(H$_2$O)}(η^4,μ-ox){*fac*-Ru(DMSO-S)$_3$(DMSO-O)}]$^{2+}$ (**17a**) and the diaquo [{*fac*-Ru(DMSO-S)$_3$(H$_2$O)}$_2$-

Scheme 10. Chemical Behavior of the Dinuclear Compound **17** in Aqueous Solution

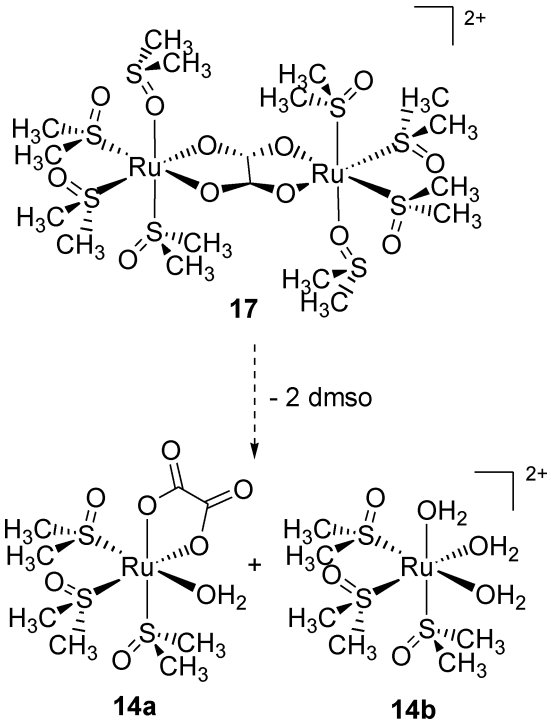

$(\eta^4,\mu\text{-ox})]^{2+}$ (**17b**) dinuclear species. This process is accompanied by the opening of the oxalate bridge leading to the formation of two mononuclear fragments, one corresponding to **14a** and the other (**14b**) bearing only water and DMSO-S ligands (Scheme 10). Addition of 100 mM NaCl to this solution (or performing the hydrolysis in 100 mM NaCl) caused, within ca. 2 weeks, the partial formation of **14** and other minor Cl-containing species. The neutral dinuclear species **15** (sparingly soluble in water) behaves similarly to **17**, even though the opening of the oxalato bridge occurs before the dissociation of the Cl ions.

Thus, we can conclude that both the oxalato bridged dinuclear species **15** and the oxalato bridged dinuclear species **17** are not stable in aqueous solution and that slow chloride/DMSO-O dissociation occurs, accompanied by a change in the coordination mode of oxalate from η^4,μ to η^2 (i.e., opening of the oxalato bridge).

The tetranuclear compound **18** was investigated at a lower concentration to avoid reprecipitation. Upon dissolution in D_2O, the six original DMSO-S methyl resonances in the ^{1}H NMR spectrum of **18** slowly decreased in favor of the three equally intense singlets of *fac*-[Ru(DMSO-S)$_3$(H_2O)(η^2-ox)] (**14a**). After 2 days, the ratio between intact **18** and **14a** was ca. 1:4 and afterward remained unchanged for over 2 weeks. During the process, the resonance of free DMSO was not observed. Thus, in aqueous solution, complex **18** partially disassembles, and on each Ru center of the tetranuclear structure, the bridging carboxylate oxygen is replaced by a water molecule (Scheme 11). Owing to the solubility problems encountered, the effect of chloride concentration on the chemical behavior of **18** was not investigated.

Scheme 11. Chemical Behavior of Tetranuclear Compound **18** in Aqueous Solution

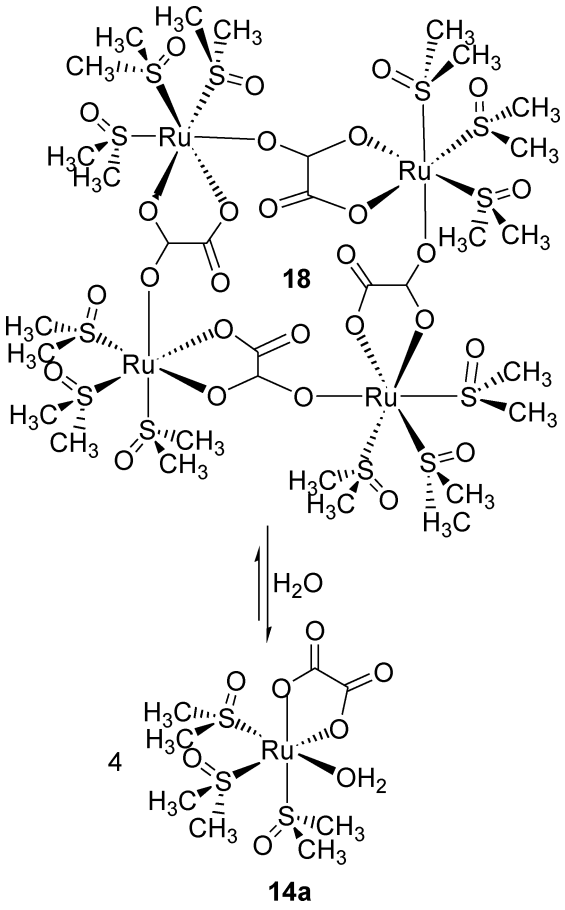

Discussion

The dicarboxylates investigated in this work have a rich coordinative behavior. Oxalate is an extremely versatile dianionic ligand as it exhibits a wide variety of coordination modes and geometries.[36] It can be monodentate, bidentate, or show both coordination modes in the same compound. The coordination mode eventually adopted by the ligand may depend, to a certain extent, also on the ratio of the reactants. The most common coordination modes with transition metals are bidentate (i.e., terminal chelate η^2, forming a five-membered ring) and bis-bidentate (i.e., bridging bis-chelate, η^4,μ) (Chart 3).[36] Oxalate binds as a chelate in the clinically approved Pt(II) anticancer complex *oxaliplatin*, [Pt(dach)(ox)]. In general, there are relatively few structurally characterized compounds in which the bridging oxalate has either one or two non-coordinated oxygen atoms (i.e., η^3,μ or η^2,μ, Chart 3).[36]

The specific bis-bidentate behavior of oxalate is forbidden to malonate and succinate by obvious steric reasons. Both malonate and succinate have a great ability to construct coordination architectures with metal ions of diverse sizes and shapes, adopting different coordination modes and geometries.[21] Malonate frequently binds to metal centers as

(36) (a) Hernández-Molina, M.; Lorenzo-Luis, P. A.; Ruiz-Pérez, C. *Cryst. Eng. Comm.* **2001**, *16*, 1−4. (b) Castillo, O.; Luque, A.; Sertucha, J.; Román, P.; Lloret, F. *Inorg. Chem.* **2000**, *39*, 6142−6144 and references therein.

Chart 3

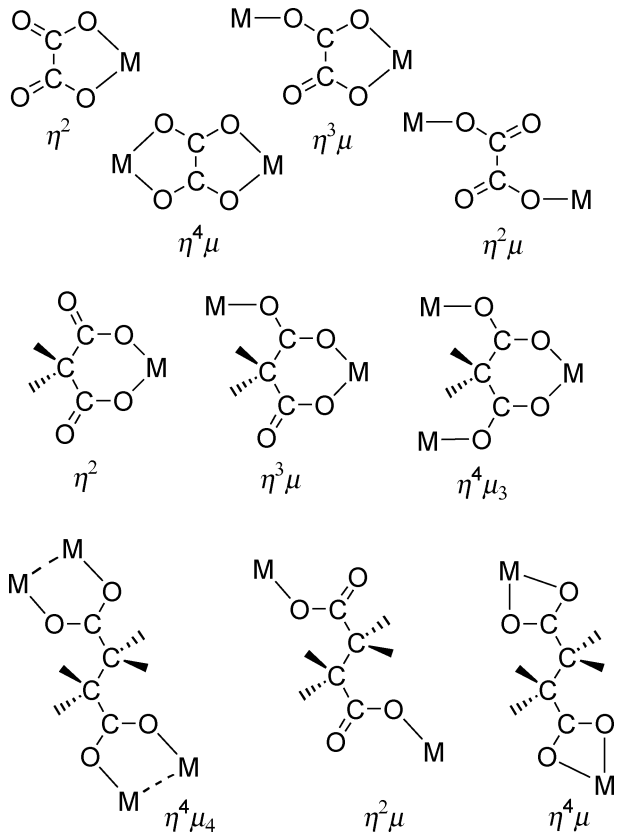

a bidentate chelating ligand (η^2), forming a six-membered ring (Chart 3). In addition, it can simultaneously act as a monodentate bridging ligand (with the unbound O atoms) toward one (η^3,μ) or two other metal centers (η^4,μ_3) (Chart 3).[37] Replacement of both protons on C^1 with methyl groups makes dmmal sterically more similar to cbdc. The chelating behavior is instead less favored for succinate, as it would produce a seven-membered ring; this ligand can behave as a bridging tetratopic connector (η^4,μ_4, tetra-monodentate), usually toward dinuclear units, but also as a bridging ditopic connector, either bis-monodentate (η^2,μ) or bis-bidentate (η^4,μ) (Chart 3).[21]

In general, few Ru complexes with potentially chelating dicarboxylates are described in the literature. As mentioned in the Introduction, there are only two Ru(II)-mal compounds known, and in both malonate acts as a chelate.[10,18] On the contrary, in the Ru(I)-carbonyl-dicarboxylate systems, malonate behaves as a tetradentate ligand bridging two dinuclear Ru units.[38] There are no previous examples of Ru-mmal and -dmmal complexes, and aside from the two compounds described by Hall and co-workers,[17] there are relatively few examples of discrete oxalato-bridged diruthenium complexes: $[\{Ru^{II}(py)_4\}_2(\eta^4,\mu\text{-ox})][BF_4]_2$,[39] $[\{(\eta^3{:}\eta^3\text{-}C_{10}H_{16})Ru^{IV}\text{-}Cl\}_2(\eta^4,\mu\text{-ox})]$,[40] $[\{Ru^{II}X(\eta^6\text{-}p\text{-cymene})\}_2(\eta^4,\mu\text{-ox})]^n$ (X = Cl, $n = 0$; X = MeOH or PPh_3, $n = 2+$; anti geometry was found),[41] and $[\{Ru^{III}(acac)_2\}_2(\eta^4,\mu\text{-ox})]$.[42] Very recently, a dinuclear Ru(II) complex with two bridging fluoro-succinato units, structurally similar to **13**, has been reported.[43]

To date, the reactivity of such dicarboxylates toward Ru(II)-DMSO precursor was largely unexplored. According to our systematic investigation, the ligands can be divided basically into two groups. The reaction of either **1** or **2** with K_2(dicarb) (dicarb = mal, mmal, ox) yielded preferentially the mononuclear species [K]*fac*-[RuCl(DMSO-S)$_3$(η^2-dicarb)] (dicarb = mal, **6**; mmal, **9**; ox, **14**) that contains a chelating dicarboxylate unit and a residual chloride. Likewise, when **3** was used as precursor, the corresponding neutral mononuclear species *fac*-[Ru(DMSO-S)$_3$(DMSO-O)(η^2-dicarb)] (dicarb = mal, **7**; mmal, **10**; ox, **16**), which contains a DMSO-O ligand in the place of Cl^-, was obtained. On the contrary, treatment of **1** (or **2**) with K_2(dmmal) and K_2(suc) yielded preferentially the dinuclear species [*fac*-Ru(DMSO-S)$_3$(H_2O)(μ-dicarb)]$_2$ (dicarb = dmmal, **11**; suc, **13**), with two bridging dicarboxylate moieties. These compounds are structurally similar to the dinuclear Ru complexes with two bridging 1,1-cyclobutane dicarboxylate (cbdc) units, [*fac*-Ru(DMSO-S)$_3$(H_2O)(μ-cbdc)]$_2$ (**4**) and [*fac*-Ru(DMSO-S)$_3$-(NH_3)(μ-cbdc)]$_2$ (**19**), previously described by us.[16] All products, regardless of their charge and nuclearity, share as a common structural feature the *fac*-Ru(DMSO-S)$_3$ fragment. Complexes with facial geometry were obtained also from **2**, implying isomerization. In addition, all the dinuclear species with bridging dicarboxylates have two water (or NH_3) molecules in anti geometry that have strong intramolecular H-bonding with the non-coordinated oxygen atoms of the carboxylate groups.

We were particularly intrigued by the different behavior of mal and cbdc: despite the structural similarity, mal prefers to bind as a chelate (η^2) on the *fac*-Ru(DMSO-S)$_3$ fragment, whereas cbdc prefers the bridging (μ) coordination mode.[16] The solid-state X-ray structural data suggested that the preferential binding mode of these dicarboxylates is dictated mainly by steric reasons. The η^2 binding mode implies that, upon formation of the six-membered chelate ring, the substituents on the central carbon atom of the dicarboxylate approach one of the two axial ligands on Ru. Malonate, with two protons on the central carbon atom, has a low steric demand and can therefore bind as a chelate. Although examples of octahedral Ru(II)[10] and Pt(IV)[44] complexes with η^2-cbdc have been reported, a boat conformation of the six-

(37) (a) Ruiz-Pérez, C.; Rodriguez-Marin, Y.; Hernández-Molina, M.; Delgado, F. S.; Pasán, J.; Sanchiz, J.; Lloret, F.; Julve, M. *Polyhedron* **2003**, *22*, 2111−2123. (b) Pasán, J.; Delgado, F. S.; Rodriguez-Marin, Y.; Hernández-Molina, M.; Ruiz-Pérez, C.; Sanchiz, J.; Lloret, F.; Julve, M. *Polyhedron* **2003**, *22*, 2143−2153.

(38) (a) Bianchi, M.; Frediani, P.; Matteoli, U.; Menchi, G.; Piacenti, F.; Petrucci, G. *J. Organometal. Chem.* **1983**, *259*, 207−214. (b) Shiu, K.-B.; Lee, H.-C.; Lee, G.-H.; Wang, Y. *Organometallics* **2002**, *21*, 4013−4016. (c) Salvini, A.; Frediani, P.; Rivalta, E. *Inorg. Chim. Acta* **2003**, *351*, 225−234.

(39) Cheng, P.-T.; Loescher, B. R.; Nyburg, S. C. *Inorg. Chem.* **1971**, *10*, 1275−1281.

(40) Steed, J. W.; Tocher, D. A. *Polyhedron* **1992**, *11*, 1849−1854.

(41) Yan, H.; Süss-Fink, G.; Neels, A.; Stoeckli-Evans, H. *J. Chem. Soc., Dalton Trans.* **1997**, 4345−4350.

(42) Fujino, T.; Hoshino, Y.; Eto, M.; Yukawa, Y.; Fiedler, J.; Kaim, W. *Chem. Lett.* **2003**, *32*, 274−275.

(43) (a) van Buijtenen, J.; Meuldijk, J.; Vekemans, J. A. J. M.; Hulshof, L. A.; Kooijman, H.; Spek, A. L. *Organometallics* **2006**, *25*, 873−881. (b) van Nispen, S. F. G. M.; van Buijtenen, J.; Vekemans, J. A. J. M.; Meuldijk, J.; Hulshof, L. A. *Tetrahedron: Asymmetry* **2006**, *17*, 2299−2305.

(44) Deng, Y.; Khokhar, A. R. *Inorg. Chim. Acta* **1993**, *204*, 35−38.

membered chelating ring induces the cyclobutane ring to sterically interfere with the axial ligands. The steric crowding can be partially relieved if η^2-cbdc adopts a half-boat or planar conformation, but these arrangements reduce the conformational flexibility of the cbdc ligand.[44] Thus, given the possibility of forming strong hydrogen bonds with one axial ligand, cbdc prefers the bridging coordination mode on octahedral complexes and forms dinuclear species. To confirm this hypothesis, we investigated also methylmalonate (mmal) and dimethylmalonate (dmmal) and found that mmal behaves like mal and binds preferentially as a chelate, while dmmal behaves like cbdc and prefers the bridging binding mode. The X-ray structures of compounds **9** and **10** (Figures 1 and 2) show that mmal can still adopt the η^2 coordination mode, with the more hindering methyl group pointing away from the crowded axial regions of each complex (equatorial conformer). This coordination is disfavored for dmmal, whose steric requirements are similar to those of cbdc and should adopt a half-boat or planar conformation to reduce steric interference with the axial ligands. Nevertheless, under appropriate conditions, we could isolate also the dinuclear species with bridging mal, [*fac*-Ru(DMSO-S)$_3$(H$_2$O)(μ-mal)]$_2$ (**8**), and the monunuclear compound with chelating dmmal, [K]*fac*-[RuCl(DMSO-S)$_3$(η^2-dmmal)] (**12**).

Similar to cbdc and dmmal, succinate behaves preferentially as a bridging ligand, and the dinuclear species [*fac*-Ru(DMSO-S)$_3$(H$_2$O)(μ-suc)]$_2$ (**13**) was the only product isolated. In this case, the chelating binding mode is disfavored because it would lead to the formation of a seven-membered ring.

Oxalate can be hardly compared to the other dicarboxylates investigated because, beside the chelating coordination mode (η^2), it has the bridging bis-chelate (η^4,μ) coordination mode available. In fact, the dinuclear species [{*fac*-RuCl(DMSO-S)$_3$}$_2$(η^4,μ-ox)] (**15**) and [{*fac*-Ru(DMSO-O)(DMSO-S)$_3$}$_2$-(η^4,μ-ox)][CF$_3$SO$_3$]$_2$ (**17**) were selectively obtained upon treatment of **1** or **3**, respectively, with 0.5 equivalent of K$_2$-(ox). The mononuclear species **14** and **16** might be capable of binding another metal center through the two peripheral oxygen atoms and thus be exploited for the preparation of unsymmetrical (and possibly heteronuclear) dimers. Work in this sense is in progress in our laboratory. Perhaps most interestingly, prolonged heating of the chloride-free precursor **3** with K$_2$(ox) yielded the tetranuclear macrocycle [*fac*-Ru-(DMSO-S)$_3$(η^4,μ-ox)]$_4$ (**18**), which features bridging monochelate oxalate moieties. This binding mode for oxalate is rare, in general, and unprecedented for Ru. Examples of structurally characterized compounds containing η^4,μ-ox ligands concern both polymeric[45] and discrete (mainly dinuclear) species.[46] Discrete oxalato-bridged tetranuclear macrocycles similar to **18** are, however, unknown. A molecular square similar to **18** with malonate in place of oxalate, [Cu(η^3,μ-mal)(2,4′-bipy)(H$_2$O)]$_4$·8H$_2$O (2,4′-bipy = 2,4′-bipyridine), was described by Ruiz-Pérez and coworkers.[37]

The chemical behavior of the new compounds in aqueous solution was investigated in view of their potential anticancer activity. While the chloride-DMSO Ru precursors **1** and **2** upon dissolution in water rapidly release one or two DMSO ligands, respectively, followed by the hydrolysis of at least one chloride,[11] most of the new complexes are relatively more inert. No dissociation of the dicarboxylate ligands, either chelate or bridging, was observed in D$_2$O. The most labile ligand was DMSO-O (when present), followed by chloride (when present). However, while DMSO-O dissociation was complete (hours), chloride hydrolysis led to equilibria (days). Thus, owing to the stability of the *fac*-Ru-(DMSO-S)$_3$ fragment, in aqueous solutions most of the new species set free only one coordination position (or up to three if they are unstable dimers). Interestingly, while the dinuclear compound with bridging mal (**8**) is unstable in aqueous solution and spontaneously evolves to the mononuclear aquo species (**6a**) with mal bound as a chelate ($\mu \rightarrow \eta^2$ rearrangement), the opposite occurs with the cbdc and dmmal complexes ($\eta^2 \rightarrow \mu$ rearrangement) in which the bridging binding mode is more stable than the chelate. The polynuclear compounds with bridging chelating oxalate, both η^4,μ (**15**, **17**) and η^3,μ (**18**), are also unstable in aqueous solution and spontaneously evolve to the mononuclear aquo species bearing η^2-ox. In the case of the dimers, the η^4,$\mu \rightarrow \eta^2$ rearrangement of ox (opening of the bridge) involves also the formation of an oxalato-free Ru-DMSO aquo species. In the hydrolysis of **18** to four *fac*-[Ru(DMSO-S)$_3$(H$_2$O)-(η^2-ox)] (**14a**) units, no intermediate species was observed, thus implying that the opening of the first oxalato bridge leads to the rapid decomposition of the whole tetranuclear molecule.

Conclusion

The aim of this work was that of preparing derivatives of Ru(II)-DMSO anticancer complexes with potentially chelating dicarboxylates (dicarb), for assessing how the nature of the anionic ligands influences the biological activity of these species. As a result of our systematic investigation, we described and structurally characterized a number of new Ru(II)-DMSO-dicarboxylate complexes (mono-, di-, and tetra-nuclear) obtained by treatment of precursors *cis*,*fac*-[RuCl$_2$(DMSO-S)$_3$(DMSO-O)] (**1**), *trans*-[RuCl$_2$(DMSO-S)$_4$]

(45) Examples of polymeric η^3,μ-oxalato compounds: (a) Geiser, U.; Ramakrishna, B. L.; Willett, R. D.; Hulsbergen, F. B.; Reedijk, J. *Inorg. Chem.* **1987**, *26*, 3750−3756. (b) Oshio, H.; Nagashima, U. *Inorg. Chem.* **1992**, *31*, 3295−3301. (c) Rochon, F. D.; Melanson, R.; Andruh, M. *Inorg. Chem.* **1996**, *35*, 6086−6092. (d) Shen, H.-Y.; Bu, W.-M.; Liao, D.-Z.; Jiang, Z.-H.; Yan, S.-P.; Wang, G.-L. *Inorg. Chem.* **2000**, *39*, 2239−2242. (e) Novosad, J.; Messimeri, A. C.; Papadimitriou, C. D.; Veltsistas, P. G.; Woollins, J. D. *Trans. Met. Chem.* **2000**, *25*, 664−669. (f) Ballester, G.; Coronado, E.; Giménez-Saiz, C.; Romero, F. M. *Angew. Chem., Int. Ed.* **2001**, *40*, 792−795.

(46) Examples of discrete η^3,μ-oxalato compounds: (a) Kansikas, J.; Pajunen, A. *Acta Crystallogr., Sect. B* **1980**, *36*, 2423−2425. (b) Chiozzone, R.; González, R.; Kremer, C.; De Munno, G.; Cano, J.; Lloret, F.; Julve, M.; Faus, J. *Inorg. Chem.* **1999**, *38*, 4745−4752. (c) Marinescu, G.; Andruh, M.; Lescouëzec, R.; Muñoz, M. C.; Cano, J.; Lloret, F.; Julve, M. *New J. Chem.* **2000**, *24*, 527−536. (d) Chiozzone, R.; González, R.; Kremer, C.; De Munno, G.; Armentano, D.; Cano, J.; Lloret, F.; Julve, M.; Faus, J. *Inorg. Chem.* **2001**, *40*, 4242−4249. (e) Costisor, O.; Mereiter, K.; Julve, M.; Lloret, F.; Journaux, Y.; Linert, W.; Andruh, M. *Inorg. Chim. Acta* **2001**, *324*, 352−358. f) Núñez, H.; Timor, J.-J.; Server-Carrió, J.; Soto, L.; Escrivà, E. *Inorg. Chim. Acta* **2001**, *318*, 8−14.

(**2**), or *fac*-[Ru(DMSO-S)$_3$(DMSO-O)$_3$][CF_3SO_3]$_2$ (**3**) with oxalate (ox), malonate (mal), methylmalonate (mmal), dimethylmalonate (dmmal), and succinate (suc). The molecular structures of 10 compounds, **6**−**11**, **13**, **15**, **17**, and **18**, were determined by X-ray crystallography. The wealth of spectroscopic and structural data obtained for the new Ru species provide insight into the preferential binding modes of these ligands on octahedral metal centers in general and stress the importance of steric hindrance and hydrogen bonding in determining the nature and geometry of the products. In particular, we can conclude that on octahedral metal centers, unhindered 1,3-dicarboxylates prefer the chelating (η^2) binding mode while, in the presence of steric hindrance on the central carbon atom, they prefer the bridging (μ) coordination mode and form dinuclear species if the metal center offers the possibility of making strong hydrogen bonds with one axial ligand. We also found that in aqueous solution, the investigated dicarboxylates are not released from the Ru center, regardless of their coordination mode. This behavior, which was anticipated for the chelating binding mode, is proven true here also for the bridging coordination mode.

In vitro biological tests for assessing the cytotoxicity of the new Ru-DMSO-dicarb complexes against murine and human cancer cell lines, in comparison with the chloride precursors **1** and **2**, are in progress and will be reported elsewhere.

Acknowledgment. Fondazione CRTrieste, Fondo Trieste, and Regione Friuli Venezia-Giulia are gratefully acknowledged for financial support. We thank Engelhard Italiana S.p.A. for a generous loan of hydrated $RuCl_3$.

Supporting Information Available: Tables of X-ray crystallographic data in CIF format for compounds **6**−**11**, **13**, **15**, **17**, and **18**; tables of intramolecular H-bond distances (Å) and angles (deg) for dinuclear compounds **8**, **11**, and **13**; X-ray structures of compounds **6**−**8**; 1-D polymeric chain of **6** in solid state; 2-D HMQC NMR spectra of **6**−**8** and **13**; possible stereoisomers of Ru-DMSO complexes with η^2-mmal; 2-D net of **9** in solid state; space filling structure of **18**; packing view of **18**; comparative view of the X-ray structures of the two conformers of **18**; 2-D HMQC spectrum of 10% D_2O solution of **6** after 6 days. This material is available free of charge via the Internet at http://pubs.acs.org.

IC0613964